DISSERTAÇÃO DE MESTRADO IFT–D.005/2024

A Study of Dense Nuclear Matter in a Meson-Nucleon Model Including Quark-Exchange Effects

Genilson Alves Cardoso da Silva

Orientador

Gastão Krein

Maio 2024

S586s

Silva, Genilson Alves Cardoso da

A study of dense nuclear matter in a meson-nucleon model including quark-exchange effects / Genilson Alves Cardoso da Silva. – São Paulo, 2024

77 f. : il. color.

Dissertação (mestrado) – Universidade Estadual Paulista (Unesp), Instituto de Física Teórica (IFT), São Paulo

Orientador: Gastão Krein

1. Estrelas de neutrons. 2. Física nuclear. 3. Matéria nuclear. I. Título

Sistema de geração automática de fichas catalográficas da Unesp. Biblioteca do Instituto de Física Teórica (IFT), São Paulo. Dados fornecidos pelo autor(a).

A STUDY OF DENSE NUCLEAR MATTER IN A MESON-NUCLEON MODEL INCLUDING QUARK-EXCHANGE EFFECTS

Dissertação de Mestrado apresentada ao Instituto de Física Teórica do Câmpus de São Paulo, da Universidade Estadual Paulista "Júlio de Mesquita Filho", como parte dos requisitos para obtenção do título Mestre em Ciências, área Física.

Comissão Examinadora:

Prof. Dr. GASTÃO INÁCIO KREIN (Orientador)
Instituto de Física Teórica/UNESP

Prof. Dr. ANA JULIA SILVEIRA MIZHER
Instituto de Física Teórica/UNESP

Prof. Dr. KAZUO TSUSHIMA
UNICID/Universidade Cidade de São Paulo

Conceito: Aprovado

São Paulo, 10 de maio de 2024.

À minha mãe, por tudo.

Acknowledgment

Primeiramente gostaria de agradecer à minha magnífica e grandiosa mãe Rosa Maria que, em absolutamente todos os momentos, tem me apoiado nessa minha grande jornada no mundo acadêmico: Desde carinho, amor e educação até a sua demonstração de ser uma pessoa extremamente dedicada e guerreira no qual tento me espelhar. Agradeço à minha namorada, companheira e amiga, Nathalia Cappellini, por ter sempre me incentivado e apoiado nessa caminhada complexa e me fez enxergar como tudo vale a pena. Aos meus familiares de São Paulo que me deram todo o apoio e acolhimento possível e necessário no inicio de meu mestrado.

Aos meus amigos de longa data que tive o prazer de conhecer no ínicio de minha graduação, Matheus, Clisman, Flávio, Daniel, Anisio, Antonio (vulgo bereu) e Valério onde até nos dias de hoje mantemos um contato sólido e, sempre que possível, nos entretemos com bons jogos e conversas discontraídas em nosso belo grupo do Survivor Royale. Gostaria também de agradecer a todos os colegas que consegui fazer no IFT, mas, em especial, ao João e Isabela, por serem excelentes conselheiros, grandes fontes de suporte emocional e, sem sombras de dúvidas, ótimas inspirações no qual me ajudou a dar uma continuadade saudável neste mestrado.

Ao Professor Bruno do IF SertãoPE, meu orientador de iniciação científica, que, por suas excelentes e motivadoras aulas de Física-Matemática, foi onde meu interesse em seguir na carreira de física teórica surgiu. Ao meu orientador Professor Gastão, um grande exemplo com quem tem sido uma honra colaborar e aprender, além de sua paciência, encorajamento e dedicação.

Agradeço à coordenação e todos os servidores do Programa de Pós-Graduação do IFT.

Por fim, agradeço à CAPES pelo suporte financeiro.

Resumo

Estrelas de nêutrons são remanescentes de supernovas. O núcleo interno de uma estrela de nêutrons é composto principalmente de matéria de nêutrons. A estabilidade da estrela se deve à atração gravitacional que é equilibrada pelo efeito combinado da pressão de degenerescência dos nêutrons e interações inter-nêutrons. Este estudo apresenta uma visão geral da fenomenologia básica das estrelas de nêutrons, incluindo alguns fatos históricos e discute as propriedades da matéria nuclear e matéria de nêutrons densas. Usamos o modelo de Walecka na aproximação de campo médio para obter a equação de estado da matéria densa de nêutrons e calcular propriedades de uma estrela de nêutrons. O modelo de Walecka é uma teoria quântica de campos relativística de mésons e núcleons, Também discutimos os efeitos da troca de quarks entre núcleons na equação de estado. Trocas de quarks surgem em densidades suficientemente altas quando os núcleons têm uma alta probabilidade de sobreposição. Nossa contribuição original é calcular as corrreções devidas a trocas de quarks em um modelo de quarks constituintes e avaliar seu impacto na equação de estado calculada com o modelo de Walecka incluindo efeitos de autointeração entre os mésons. Examinamos como essas correções à equação de estado podem afetar propriedades fundamentais de estrelas de nêutrons, como massa, raio e rigidez.

Palavras Chaves: Estrela de Nêutrons; Teoria de Campos Térmicos; Matéria Nuclear Densa;

Áreas do conhecimento: Física; Fisica nuclear e de Campos;

Abstract

Neutron stars are remnants of supernovae. The inner core of a neutron star is composed mainly of neutron matter. The stability of the star is due to the attractive gravitational force which is balanced by the combined effect of the degeneracy pressure of the neutrons and interneutron interactions. This study presents an overview of the basic phenomenology of neutron stars, including some historical events, and discusses the properties of dense nuclear matter and pure neutron matter. We use the Walecka model in the mean field approximation to obtain the equation of state of dense neutron matter and compute properties of a neutron star. The Walecka model is a relativistic quantum field theory of mesons and baryons. We also discuss the effects of quark exchange between nucleons on the equation of state. Quark exchange arises at sufficiently high densities when the nucleons have a high overlap probability. Our original contribution is to compute quark exchange corrections in a constituent quark model and evaluate their impact on the equation of state computed in the Walecka model including meson self-interactions. We examine how such corrections to the equation of state might affect fundamental properties of neutron stars, such as mass, radius, and stiffness.

Key Words: Neutron Star; Thermal Field Theory; Dense Nuclear Matter;

Knowledge areas: Physics; Nuclear and Field Physics;

Contents

Chapter 1

Introduction

The existence of neutron stars represents a fascinating cosmic phenomenon resulting from the ultimate fate of massive stars. These stars, which are remnants of supernovae, offer valuable insights into the extreme physics governed by unimaginable pressure and baryon densities. Their unique properties, such as intense magnetic fields and rapid rotations, challenge our conventional understanding of matter and the extreme conditions of the universe.

The concept of a neutron star is intrinsically linked to the stellar life cycle. We understand that stars are born from clouds of gas and dust, and their evolution can lead to the formation of neutron stars. During the birth phase, massive stars collapse under the influence of gravity, triggering nuclear reactions that sustain the star and maintain a delicate balance between gravitational force and resulting pressure. However, when the star consumes all its nuclear fuel, the balance is disrupted, leading to uncontrolled gravitational collapse.

The extreme densities found in neutron stars, with values on the order of 10^{14} g/cm^3, characterized by unique features such as intense magnetic fields of the order of 10^{12} G and extremely rapid rotations, imply relativistic conditions that demand precise descriptions by theories of special and general relativity. The physics of these stars is explored in detail in the literature, with advanced theoretical models providing insights into the relationships between mass and radius of these compact objects.

Determining the upper mass limit for neutron stars has been the subject of intensive study. Theoretical studies such as by Rhoades and Ruffini [1], have established a limit around 3.2 $M_\odot$, regardless of the equation of state. However, new research has explored large masses driving interest in ultracompact stars ([2], [3]).

The history of neutron star physics traces back to pioneering contributions by Landau, Baade, and Zwicky in the early 20th century. Theoretical understanding of these objects has been enhanced by developments such as the TOV equation by Tolman, Oppenheimer, and Volkoff [4] and investigations into stellar oscillations by

Chandrasekhar and Ferrari [5]. The observations of pulsars in the 1960s provided the first direct observational evidence of neutron star [6], [7]. The advent of the era of gravitational waves, culminating in the detection of events like GW 170817 and GW 190814 [8], has brought a new dimension to the research of ultracompact stars.

As we move into the future, the study of ultracompact stars continues to evolve. New technologies, such as the Kamioka Gravitational Wave Detector (KAGRA), promise to open new windows of observation, while theoretical investigations explore a variety of exotic compact objects and their observational effects [9]. The detection of gravitational echoes and studies on their origins offer an exciting perspective for the field [10, 11, 12]

In addition to these observationally inferred properties, the theoretical modeling of neutron stars has evolved significantly. Recent developments in theoretical physics have sought to provide a deeper understanding of the dense baryonic matter that constitutes neutron stars. Particularly, these models explore how such matter behaves under the extreme conditions present within neutron stars, linking microscopic interactions to macroscopic observables like the mass-radius relation.

Theory developments for dense baryon matter occurred in the context of density relativistic density functional theory build on the premisses of effective field theories [13]. The main purpose of a density functional theory is to provide a unified view that encompasses a variety of physical phenomena, ranging from the properties of individual nuclei to the structure and dynamics of neutron stars. Thus, considering that extrapolation to inaccessible regions in laboratory experiments is inevitable, predictions from a microscopic theory must be accompanied by properly quantified theoretical uncertainties [14, 15]. Historically, relativistic models of nuclear structure were based on renormalizable field theories, centered around renormalizability as a key requirement [16, 17]. However, a modern perspective suggests that relativistic models, while influenced by Quantum Chromodynamics (QCD), should be treated as effective field theories (EFTs), where renormalizability in the traditional sense is no longer a requirement [13]. In this approach, an EFT is designed to describe low-energy physics without detailing behavior at short distance scales. Density Functional Theory (DFT), pioneered by Kohn and collaborators [18, 19, 20] in the realm of nonrelativistic many body theories, provides a unified framework for developing an EFT capable of analyzing phenomena across various distance scales. In other words, although QCD offers a deeper description of strong interaction and could be a valuable tool in understanding neutron stars, its highly nonlinear nature at the hadronic energy scale makes direct theoretical calculations infeasible. This leads us to search for a model grounded in an EFT that can capture the phenomenological characteristics of nuclear matter.

We understand the importance of understanding the behavior of baryons in dense and highly interactive environments, as well as the properties resulting from dense baryonic matter. These issues arouse great interest due to their role in understanding the internal structure of neutron stars, as well as in heavy ion collision experiments in the NICA-FAIR energy range. One of the key questions that requires deeper theoretical formulation and more precise understanding is how to deal with the baryon in a bound state of quarks. It is anticipated that at a critical density, the system of many baryons will undergo a change of character and turn into a new state of deconfined quarks and gluons. However, before this transition occurs, the effective interaction between baryons will be significantly modified due to the composite nature of the nucleons. Among others, a prominent effect is quark exchange between different baryons driven by the Pauli exclusion principle [21, 22, 23, 24, 25, 26, 27, 28]. Quark exchange between two baryons is a precursor phenomenon to the transition to fully deconfined quark matter. It requires consideration of two-nucleon correlations which, within a quark-model viewpoint, involves a six-quark wave function representing a partial delocalization of quarks. As such, its consideration requires going beyond the independent-particle, low-energy mean-field description of nuclear matter.

Our primary aim in this dissertation is to present a review on the properties of neutron stars. We also make an original contribution to the field by evaluating the contribution of quark exchange to the equation of state of dense baryonic matter. Our approach utilizes a relativistic field theory for baryonic matter based on the Walecka model with nonlinear scalar meson self-interactions and a constituent quark model to incorporate quark exchange effects. Our aim is to quantify the impact of quark exchange on the properties of dense baryonic matter and its consequences on the mass-radius relation of a neutron star. Although such effects have been estimated previously in the context of the traditional Walecka model, our work is the first one to estimate such effects using the nonlinear scalar self-interactions in that model. We find a very interesting result that quark exchange has opposite effects in the Walecka model and in the Walecka model with scalar self-interactions: in the first model, it decreases the pressure, whereas in the latter model it increases the pressure. This is an interesting feature because a stiffer equation of state, rising rapidly with a density around 2.4 times the normal nuclear matter saturation density, seems to be required [29] to accommodate the recent NICER measurement of the radius of the neutron star PSR J0740 + 6620 [30]. That density is in the regime where it is expected that hadronic matter transforms into quark matter.

Throughout the dissertation, we use particle physics natural units, in that $\hbar = c = k_B = 1$, where k_B is Boltzmann's constant. This study is divided into five chapters. Following a brief introduction with literature review, Chapter 2 will provide an exposition on the discovery, observations, properties, and structure of neutron stars. Chapter 3 will present some basic properties of dense nuclear matter within the Walecka model. In Chapter 4 we incorporate quark exchange effects in the Walecka model including scalar meson self-interactions. We obtain explicit numerical results for the equation of state of nuclear and pure-neutron matter. We additionally solve numerically the Tolman-Oppenheimer-Volov equation to quantify quark exchange effects on the mass-radius of a neutron star. We conclude in Chapter 6 with brief final remarks and present future prospects.

Chapter 2

Compact stars

It is undeniable the uniqueness of neutron stars, remarkable celestial bodies for their magnetic field intensity, rotation speed and matter density. A neutron star is one of the most compact astrophysical objects in the universe and its extreme attributes challenge the limits of physics. In this chapter, we will explore the history and evolution of knowledge about neutron stars, addressing fundamental aspects ranging from their discovery to their theoretical and observational charcterization.

To begin, in Section 2.1, we trace the path of the discovery of neutron stars. From the earliest observations that suggested their existence to the most recent investigations , we explore the process by which these celestial bodies were identified and understood by the scientific community. We will also discuss the historical milestones and key contributions that have shaped our current understanding of these fascinating objects.

An interactive way to approach this topic is through Figure 2.1, which serves as a valuable resource to situate our research within the current stage of scientific development in the field that presents a crucial element in the study of stars in general and particularly neutron stars. Therefore next in Section 2.2, we will describe a bit about the properties and structures of neutron stars such as their composition and the equation that dictates the relationships between pressure and the density of matter - Equation of State (EoS). Finally, in Section 2.3, Let us clarify some topics regarding observational data and we also analyse the latest discoveries and advancements in this area and discuss their implications for modern physics and astrophysics.

2.1 Discovery

After the remarkable discovery of the neutron by Chadwick in 1932, Baade and Zwicky, the following year, conceived the intriguing idea of neutron stars while

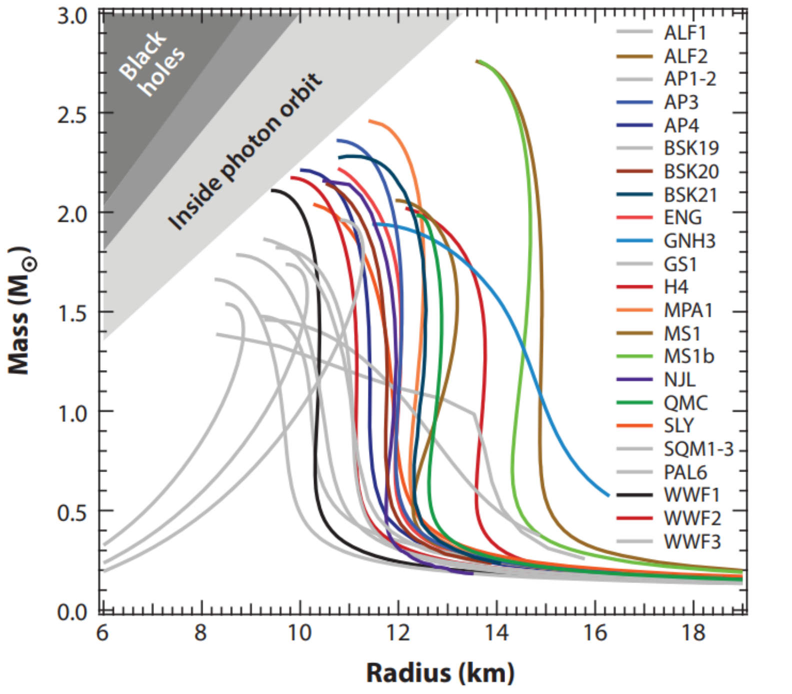

Figure 2.1: Mass-radius diagram of neutron stars for a variety of equations of state. Refer to Ref. [31], from which the figure was taken, for descriptions of the equations of state, acronyms, and other references.

investigating supernovae. The question that intrigued them was: What source could suddenly release so much energy, making stellar explosions visible even in daylight, and hurling stellar remnants at extraordinary speeds into space? They suggested that the answer lays in the gravitational binding of a highly compact object formed from the central core of a star about to explode.

However, despite the insight of Baade and Zwicky, little attention was immediately given to the search for neutron stars after the publication of their paper. At that time, there simply was not a clear understanding of what to look for. A compact star composed of densely packed neutrons was believed to be degenerate, incapable of generating energy after its formation, and its visual detection was considered impossible due to its tiny size compared to white dwarfs. Other forms of radiation also seemed unpromising.

It was only in 1939, years before the discovery of pulsars, that Oppenheimer and Volkoff [4] and Tolman [32] were the first to take seriously the question of the structure of the compact objects predicted by Baade and Zwicky. They estimated that such objects would have a radius of about ten kilometers and a maximum mass of approximately 3/4 of the solar mass. These calculations were followed by other speculations, such as Woltjer's proposal in 1940 that the conservation of magnetic flux could lead to the existence of intense magnetic fields in neutron stars reaching 10^{12} G [33].

Meanwhile, in Cambridge, Anthony Hewish had developed a radio telescope with fast response capability, intended to study the scintillation of point radio sources. It was through this telescope that his student, Jocelyn Bell, in 1967, first detected the periodic radio signals of a pulsar, located outside the solar system. Later, thirty-four years after Baade and Zwicky suggested that the source of energy capable of driving a supernova would be the gravitational binding of a neutron star, Hewish, Bell, Pilkington, Scott, and Collins [6] published their discovery. They had identified a very discrete source of pulsating radio signal located outside the solar system, possibly a condensed star, a white dwarf, or a neutron star. The first pulsar had been found.

The discovery of the first pulsar was just the beginning. Quickly, other pulsars, such as those in the Crab Nebula and Vela, were identified, and in the following decades, more than 250 others were discovered in large astronomical surveys. The term "pulsar" was coined to describe these objects, which emit pulsed radiation extremely regularly, and which became known as the observable versions of neutron stars. The University of Cambridge states that, to date, over 3,000 pulsars have been discovered and, although initially found in radio waves, we have since discovered these cosmic beacons in X-rays, gamma rays, and even visible light.

While it is widely accepted that pulsars are indeed neutron stars, it is important to distinguish between the two terms. "Pulsar" is reserved to describe the astrophysical object that emits pulsed radiation, while "neutron star" refers to the theoretical object, regardless of its detection as a pulsar or by other means. For example, the partner of the Hulse-Taylor pulsar [34] is inferred to be a neutron star based on indirect observations, although not detected as a pulsar. In this case, its existence is inferred through the Doppler shift caused by orbital motion when pulses are received from the observed pulsar. From the observations, the mass and orbital parameters deduced indicate that the invisible partner is highly compact, strongly suggesting it to be a neutron star rather than a white dwarf. However, the companion could also be a pulsar. If so, the Earth would not be in the cone swept by the radio emission along the magnetic dipole as the star rotates.

From the early theorizations about neutron stars in the 1930s to the observational discoveries of pulsars, many scientists have contributed to the understanding of this astrophysical phenomenon. Oppenheimer, Volkoff and Tolman established the theoretical foundations [4, 32]. The interpretation of this discovery as a highly magnetized neutron star was already present in Pacini's article [35] when, in 1967, Hewish and Bell identified the first pulsar. Furthermore, Gold's article [36] also reinforced the association between pulsars and neutron stars. The likely existence of hyperons in neutron stars was recognized by Cameron [37]. Pandharipande [38], Bethe and Johnson [39], and Moszkowski [40] introduced hyperons in a Schrödinger potential approach for constituent interactions. Further studies have emphasized the populations of hyperons in neutron stars and their impact on pulsar observations, such as the mass limit [41, 42, 43]. The complex interplay between hyperons and observables was addressed in [44]. These works also emphasized the importance of constraining theory through various properties of nuclear matter [45, 46]. Hybrid stars, representing a mixture of hadronic matter and quarks, are well-analyzed in these articles [47, 48]. The fascination with these compact objects continues to drive astronomical research to this day.

2.2 Properties and structure of neutron stars

Neutron stars form from the gravitational collapse of interstellar clouds, giving rise to a proto-star that initiates nuclear fusion. After depleting their fuel, massive stars can explode in supernovae, leaving behind a neutron star or, in extreme cases, a black hole [49]. These stars are incredibly compact, with up to 2 $M_{\odot}$ compressed into a space of just 10 Km. Once formed, the neutron star undergoes a stabilization process, reaching a favorable energy state for the system. Various reactions occur until the star reaches a degenerate state, where no more nuclear reactions take place. After releasing all internal heat, the star enters a fundamental state of electrically neutral matter. At this point, its composition stabilizes, obeying physical laws such as the conservation of chemical potential and charge. Despite the name 'neutron star', these stars are not composed solely of neutrons, as this would not constitute the lowest energy state. Neutrons decay into protons and electrons through beta decay, and other reactions occur depending on the depth and density of the object. Thus, the composition of neutron stars can vary, from atoms to quarks. This section aims to explore succinctly the composition and structure of neutron stars, as well as discuss the equations of state that describe these objects.

2.2.1 Composition

A neutron star is expected to exhibit various phases of dense and highly interactive matter, making the description of its composition a challenging and intriguing task. An approach consistent with the physics of the object is to divide it into layers, allowing us to better understand its internal structure. In Figure 2.2, we present a schematic representation of the different regions of a neutron star, highlighting the importance of the crust, which is located just below the envelope. The crust is subdivided into an outer layer and an inner layer, each playing a crucial role in understanding the dynamics and physics of this object. The outer crust begins around 10^4 g/cm^3 and has a thickness of a few hundred meters. In this region, atomic nuclei are arranged in a body-centered cubic (bcc) lattice structure, immersed in a sea of electrons that become relativistic at densities of approximately 10^7 g/cm^3 [50]. It is in this extremely dense environment that protons and neutrons remain bound in atomic nuclei. The equilibrium nucleus in this region is predominantly composed of ^{56}Fe, which is the end result of stellar nucleosynthesis. However, the specific properties of iron under these extreme conditions of density, pressure, and temperature found inside a neutron star are still a mystery, requiring the use of theoretical models for further analysis. As we move deeper into the star, equilibrium nuclei become increasingly enriched with neutrons due to the ionization of atoms caused by intense gravitational pressure. This phenomenon culminates in a critical point, where the chemical potential of neutrons surpasses their rest masses, triggering the so-called "neutron drip point". This point marks the boundary between the outer crust and the inner crust of the neutron star, delineating a fundamental transition in the structure of this cosmic object [51].

The inner crust of the neutron star, under the intense gravitational field, is composed of neutron-rich nuclei organized in a bcc structure, coexisting with dripped neutrons and uniform electrons. With a thickness of about 1 km, this region witnesses the gradual release of neutrons from the nuclei as density increases. At the boundary between the crust and the core, the nuclei dissolve into uniform nuclear matter. Moving into the core of the neutron star, which harbors approximately 99% of its total mass, interactions between particles are dominated by nuclear physics, and observable properties of nuclear matter are considered, primarily based on effective field theories. In the upcoming chapters, we will delve deeper into these concepts and also discuss other models that seek to describe the

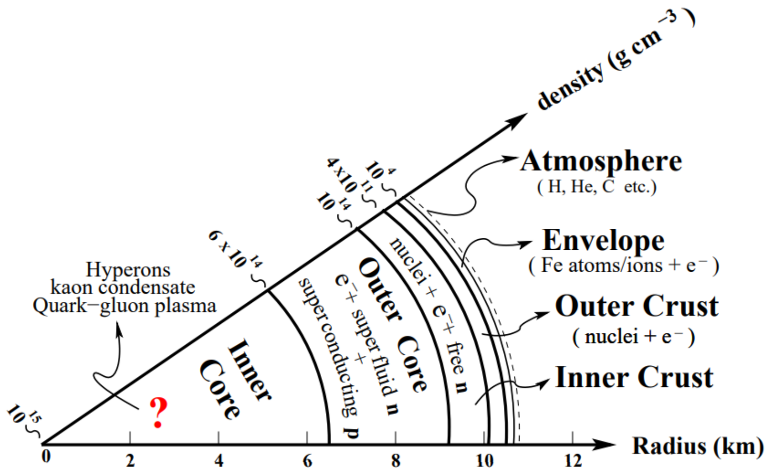

Figure 2.2: Schematic structure of a neutron star interior; figure taken from Ref. [50].

neutron star core..

2.2.2 Equations of state

When matter is compressed beyond the nuclear saturation density ρ, it ceases to exist in the form as we ordinarily know it. New forms of matter structure emerge, challenging existing fundamental physical theories and demanding more detailed explanations. On Earth, even the most powerful laboratories and particle accelerators cannot reach the necessary density to study this type of matter. Therefore, physical objects like neutron stars provide a unique opportunity for such studies. The approach to understanding this phenomenon involves dealing with equations of state (EoS), which describe the relationship between pressure and matter density in a specific system, taking into account the microphysical interactions among particles. For a neutron star, it's essential to describe the theoretical model considering nuclear physics and the various interactions among particles, thus obtaining an EoS. Then, using hydrostatic equilibrium equations, such as the Tolmann-Oppenheimer-Volkov (TOV) equations based on general relativity, it's possible to solve the problem for a given central density, thus allowing us to predict the mass and radius of the object.

It is worth highlighting some important general properties of the EoS. It is observed that each EoS predicts a maximum central density, beyond which no stable stellar configuration is possible, resulting in a maximum mass for neutron stars. Additionally, an EoS can be interpreted as a measure of the compressibility of matter, as it describes pressure as a function of the density of a physical object. The higher the pressure required for a given density, the lower the compressibility of the object. This means that an EoS with higher pressure compared to another indicates that the matter described by it is less compressible; examples of this can be observed by examining all points of the pressure-density relation (figure 2.3). Therefore, when we say that an EoS is stiffer than others, we are referring to the fact that the matter described by it is less compressible, while softer EoSs are associated with more compressible materials. In neutron stars, this implies that softer EoSs result in neutron stars with smaller maximum masses than stiffer EoSs.

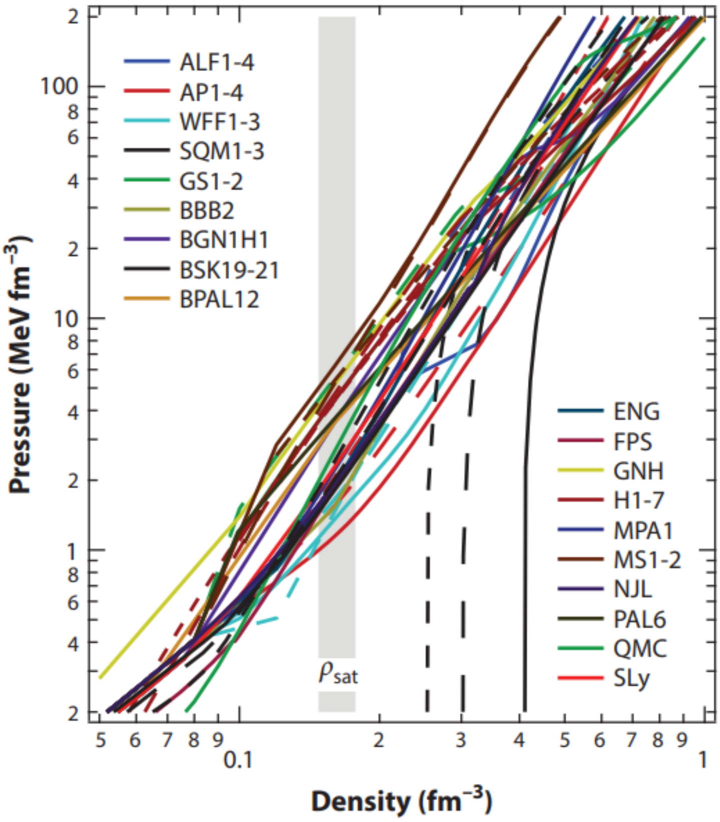

Figure 2.3: Samples of EoS calculated based on different physical assumptions. Refer to [31] for descriptions of the equations of state, acronyms, and other references.

2.3 Observations

So far, we have discussed the importance of observations in studying neutron stars several times, albeit superficially. In this section, our aim is to provide a brief and concise overview of the main methods of observational study of neutron stars, ranging from observing the pulsations of pulsating radio sources (pulsars) to the latest advances in the field of gravitational waves.

We have already discussed that the formation of neutron stars occurs after the collapse of a main sequence star in a supernova explosion. From a star with a radius of approximately 10^6 Km, an extremely compact object emerges , with a radius of about $10 - 12$ Km. During this process, to ensure the conservation of angular momentum and magnetic flux, both the rotation magnitude and the magnetic field intensity must increase significantly. Due to the unpredictability of the supernova explosion, it is not reasonable to expect the rotation axis and the magnetic field axis to coincide after the event. In fact, this alignment does not occur, and it is this misalignment between the magnetic and rotation axes that allows us to observe neutron stars. This phenomenon results in the emission of radiation pulses from the magnetic axis, which constantly sweep through space in the form of a cone, in an effect known as the "lighthouse effect." Thus, if by chance we are in the direction swept by this cone, we will be regularly exposed to the light from the neutron star, observing its pulsations consistently, pulse after pulse.

In fact, this radiation is emitted due to the intense magnetic field of the neutron star, combined with its high rotation speed on the surface. This configuration results in a Lorentz force that accelerates charged particles towards the surface of the star, creating an electromagnetic beam that flows through the poles of the magnetic field. This phenomenon is responsible for the emission of the pulsations that we observe. Additionally, the misalignment between the magnetic and rotation axes causes the magnetic dipole to apply torque to the star, causing a loss of rotational energy and a consequent increase in the object's rotation period. Although this increase is small, on the order of 10^{-15} s/s, it is observable and constant, unless glitches occur, which are sudden and inconsistent changes in the rotation frequency of a pulsar. This constant increase in the rotation period serves as an additional argument to establish that pulsars are indeed neutron stars. Otherwise, one could argue that the pulsations occur due to vibrations of the object, not due to rotation. However, if that were the case, only the amplitude of the vibration would be affected, keeping the frequency constant. This is just one of several indications and pieces of evidence that support the association between neutron stars and pulsars [49].

Due to the limitation in detecting pulsar radiation in locations further from Earth, most observed pulsars are located within our own galaxy, the Milky Way. So far, as previously mentioned, over 3000 pulsars have been identified, the majority of which reside in this galaxy. The discovery of these pulsars is associated with key parameters, including their rotation period (P), their measured dispersion (MD), which is related to the density of free electrons along the line of sight between the pulsar and Earth, and their position in the sky. It is no wonder that millisecond pulsars (MSPs), in particular, are considered the "cosmic clocks" of the universe, as their rotation periods can be determined with extraordinary precision, up to 15 significant figures after long-term monitoring. This exceptional precision allows for detailed characterization of other parameters of the object. Furthermore, the techniques used to measure these periods with high precision can also be employed to test the theory of general relativity under conditions of strong gravitational fields, especially in binary systems involving white dwarfs and neutron stars, or even two neutron stars. A notable example is the binary system PSR J0737–3039, which provides one of the best tests of general relativity to date, confirming Einstein's predictions with an accuracy of 0.05% [51]. It is important to highlight that MSPs are objects characterized by rapid rotation, weak magnetic fields, and advanced ages. Originally, these pulsars were classified as recycled pulsars due to their peculiar rotation profile. However, it is now widely accepted that these MSPs are part of a recycling scenario, in which the rotation of neutron stars is accelerated during the phase of low-mass X-ray binary (LMXB). During this phase, the neutron star, which is the older and less magnetized component of the binary system, accretes matter from its low-mass companion. This process, known as accretion, occurs at relativistic speeds, resulting in the acceleration of the star's rotation to millisecond periods. Interestingly, studies suggest that, depending on the equation of state (EoS), only a small fraction of solar mass ($0.1 - 0.2 M\odot$) is sufficient to accelerate the rotation of the object to the short periods typical of an MSP [51].

On the other hand, there are pulsars that stand out for the extreme intensity of their magnetic fields. Known as magnetars, these strongly magnetized pulsars exhibit rapid variations in their properties and radiative behaviors. It is believed that the intensity of the magnetic field is the cause of these variations, affecting the pulsar's crust and magnetosphere and resulting in thermal changes and energy emission visible to us. Historically, magnetars have been associated with two distinct groups: Anomalous X-ray Pulsars (AXPs), which show luminosity higher than expected for common X-ray pulsars, and Soft Gamma-ray Repeaters (SGRs), which demonstrate variations in their gamma-ray or X-ray emissions. Measurements of rotational slowdown revealed the presence of intense magnetic fields in both groups, in the range of $10^{14} - 10^{15}$ G. Subsequently, additional observations highlighted the similarities between SGRs and AXPs, leading to the unification of these classes under the concept of magnetars. The radiative variations observed in these objects can be categorized into bursts, outbursts, and giant flares. The first two are associated with rapid changes in the magnetic field structure, while the latter is linked to events on a more global scale within the object. All of these events release significant amounts of stored energy, reaching up to 10^{46} ergs in a single second in the case of giant flares. Detailed modeling of these events is performed through high-performance numerical simulations, combining previously developed analytical and semi-analytical models in Ref. [51].

As discussed in the previous section, obtaining accurate measurements of mass and radius is crucial for delineating important constraints in the construction of Equations of State (EoS's). Observations across various ranges of the electromagnetic spectrum contribute to these measurements, but radio emissions are especially reliable for mass measurements. Binaries, such as double neutron star systems (DNS) and millisecond pulsar with white dwarfs (MSP-WD) systems, provide precise measurements due to their measurable orbital motions. However, the masses of isolated pulsars cannot be directly determined as measurement methods are generally associated with the orbital motions of the systems [31]. Figure 2.4 illustrates mass measurements of various neutron stars, categorized by different types. It is evident that the main mass range of these objects varies from approximately approximately 1 to 2 solar masses. As for radii, the measurements are numerically smaller and more dependent on models, exhibiting greater uncertainty compared to precise mass measurements. However, in recent years, significant progress has been made in obtaining measurements of radius and mass through thermal emissions from low-mass X-ray binaries (LMXBs) [51]. It is important to note that, although not quantitatively significant, combinations of mass and radius measurements of the most massive neutron stars already impose some constraints on the Equations of State describing matter significantly denser than nuclear density.

Regarding the maximum mass of neutron stars, it has long been recognized that a limit is established based on certain theoretical assumptions. For example, based on the analyses of Rhoades and Ruffini [1], Glendenning [49] determined a maximum mass value of $3.14M\odot$ (along with a less restrictive value of $4.30M\odot$). However, as discussed in the previous section, the maximum mass still theoretically depends on various properties of the star, from its composition to the arrangement of matter. From an observational standpoint, a clear limit has always been set around $2.0 - 2.1 M\odot$. As shown in Figure 2.4, the most precise measurement at that time was that of the recycled pulsar J0348+0432, with a mass of $2.01 \pm 0.04 M\odot$. Currently, the most accurate measurement is of the star PSR J0740+6620, a neutron star in a binary system with a white dwarf, confirmed as a millisecond pulsar, with a mass of $2.14^{+0.20}_{-0.18} M\odot$ [52] (later refined to $2.08 \pm 0.07 M\odot$ [30]). Additionally, objects with even larger masses than this have been recently detected through analyses of compact object merger events via gravitational waves.

Finally, it is crucial to dedicate a space to highlight the observational advances resulting from the highly significant direct detection of gravitational waves. Initially, all gravitational wave detections were related to binary black hole systems. It was only in 2017 that the first detection of gravitational waves associated with a binary neutron star system occurred [8], a milestone that indirectly confirmed the existence of gravitational radiation years earlier [53]. The formation of a binary neutron star system can occur in various ways, from direct formation to dynamic capture, which occurs in denser regions such as globular clusters. When the binary system is compact enough, fusion is expected to occur due to the dissipation of angular momentum through the emission of gravitational radiation. This fusion represents an incredibly rich process in terms of physical information, given the extreme situation already evidenced in neutron stars, now amplified with even more complex microphysics, a diverse range of electromagnetic processes, and even more intense gravitational fields. In August 2017, the advanced detector network LIGO and Virgo detected the signal of the inspiral followed by the merger of the binary neutron star system GW 170817. Simultaneously, various observatories around the world confirmed the association of this merger with a GRB (GRB 170817A) through correlated electromagnetic detections. Restricting certain physical parameters, Abbott et al. [8] estimated the total mass of the system to be $2.74^{+0.04}_{-0.01} M\odot$, with estimates of the individual masses of the stars in the range of $1.17 - 1.60 M\odot$. An important consequence of these mergers is that their dynamics, including waveforms, merger discs, timescales, and electromagnetic emissions, sensitively depend on the mass, radius, and composition of the objects involved, suggesting a possible use of this data to constrain equations of state and thus the entire extreme physics associated with them. Furthermore, it is important to note that the observation of gravitational waves emitted by isolated neutron stars is expected in the near future, although this is more challenging due to the signals not being as intense as those from binary systems. However, this observation would open up even greater possibilities for investigating compact stars through gravitational wave astronomy [51].

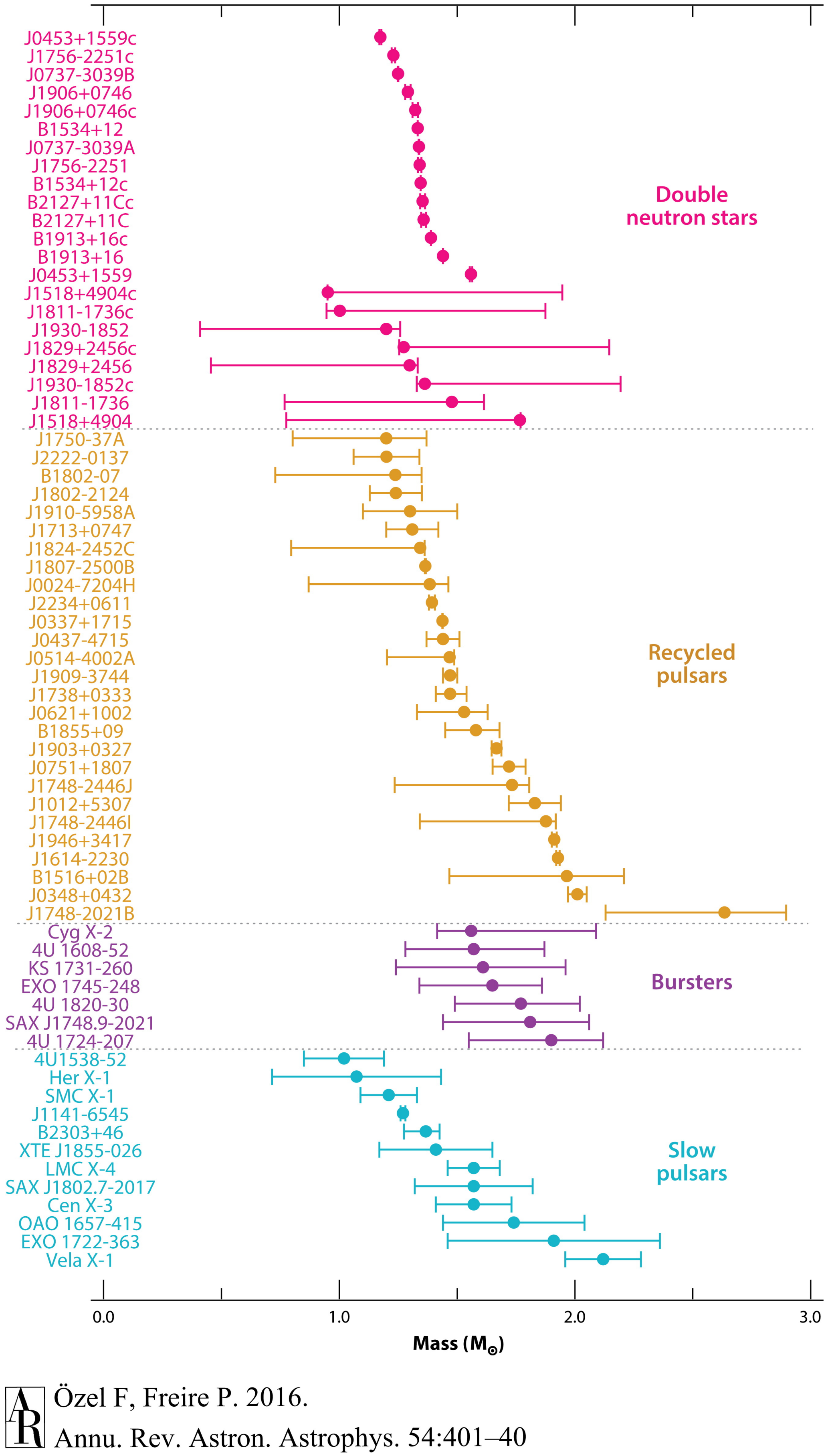

Figure 2.4: Known masses of some neutron stars; data up to 2016 [31].

Chapter 3

Basic Properties of Dense Nuclear Matter

In this chapter, we will discuss some basic properties concerning compact stars, such as their mass and radius. In this chapter, we follow closely the presentation in Ref. [54]. We begin by attempting to build an extremely simple star using only A nucleons, each with a mass of approximately 938 MeV and a with a distance scale $r_0 \simeq 0.5 \times 10^{-13}$ cm, a scale at which the inter-nucleon interaction becomes repulsive. This scale covers a volume of approximately $r_0^3 A$, which leads to a radius

$$R \sim r_0 A^{1/3} \tag{3.1}$$

and a mass

$$M \sim mA \tag{3.2}$$

Now, from the gravitational stability limit $R = 2MG$, where R is the Schwarzshild radius and G Newton's gravitational constant, we have

$$A \sim \left(\frac{r_0}{2MG}\right)^{3/2} \sim 2.6 \times 10^{57} \tag{3.3}$$

This is the maximum number of nucleons that can be added to the star before it becomes unstable. We can substitute the limiting value of A back into the expressions for the star's radius and mass, yielding:

$$R \sim 7 \text{ km}, \quad M \sim 2.3\ M_{\odot} \tag{3.4}$$

adding more nucleons would cause the star to exceed its stability limit, making it overly massive relative to its radius.

Let us perform a simple analysis indicating that relativistic effects cannot be ignored, as the Schwarzschild radius will represent a substantial portion of the star's radius. We can make an estimate of the gravitational energy E_{grav} of the star by calculating the mass of a thin spherical layer at a given radius

$$dm = \rho(r)dV \tag{3.5}$$

with $dV = 4\pi r^2 dr$ is the volume of the thin spherical layer at radius r. Suppose that the density of the star is constant, $\rho(r) = \rho$, and let $m(r)$ be the mass of the star within a spherical volume with radius $r \leq R$; then $m(r) = \frac{4\pi}{3} r^3 \rho$ and

$$E_{grav} \simeq \int_0^R G\frac{m(r)dm(r)}{r} \simeq \frac{3}{5}\frac{GM^2}{R} \simeq 0.12\ M \tag{3.6}$$

In this context, realistic values are taken as $M \simeq 1.4\ M_\odot$ and $R \simeq 10$ km. Consequently, the gravitational energy of the star constitutes more than 10% of its mass. This implies that an equation for the mass-radius relation that incorporates general relativity effect is necessary.

Next, we derive the equation that gives the mass-radius relation with Newtonian gravitation. We start by considering equilibrium between the gravitational force and the force due to pressure from the matter inside the star. In case of compact stars, this pressure includes contributions from the Fermi pressure and strong nuclear (or quark-gluon) interactions. At a given radius r, the differential pressure dP is related to the gravitational force dF as follows:

$$dP = \frac{dF}{4\pi r^2} \tag{3.7}$$

with

$$dF = -G\frac{m(r)dm}{r^2} \tag{3.8}$$

Combining these two equations and using for the energy density $\epsilon(r) = \rho(r)$ (in units $c = 1$), yields the two coupled differential equations:

$$\frac{dm}{dr} = 4\pi r^2 \epsilon(r) \quad ; \quad \frac{dP}{dr} = -G\frac{\epsilon(r)m(r)}{r^2} \tag{3.9}$$

To obtain a closed set of equations, one needs a relationship between the energy density ϵ and the pressure P, which is the equation of state (EoS). We discuss models for the EoS in the following sections. The equation for the pressure receives corrections from general relativity, leading to the Tolman-Oppenheimer-

Volkov(TOV) equation [54]:

$$\frac{dP}{dr} = -G\frac{\epsilon(r)m(r)}{r^2}\left[1+\frac{P(r)}{\epsilon(r)}\right]\left[1+\frac{4\pi r^3 P(r)}{m(r)}\right]\left[1-\frac{2Gm(r)}{r}\right]^{-1} \tag{3.10}$$

3.1 Nointeracting Nuclear Matter

Let us first consider an oversimplifield model for the EoS by neglecting all interactions. In this case, all we need is basic statistical physics and thermodynamics. The thermodynamic potential for the grand-canonical ensemble can be expressed as:

$$\Omega = E - \mu N - TS \tag{3.11}$$

where we have the energy E, chemical potential μ, particle number N, temperature T, and entropy S. The pressure is given by

$$P = -\frac{\Omega}{V} = -\epsilon + \mu n + Ts \tag{3.12}$$

where V is the volume of the system. The number density $n = N/V$, energy density $\epsilon = E/V$, and entropy density $s = S/N$. For a spin-1/2 fermionic system, these quantities are given by:

$$n = 2\int \frac{d^3k}{(2\pi)^3} f_k \tag{3.13}$$

$$\epsilon = 2\int \frac{d^3k}{(2\pi)^3} E_k f_k \tag{3.14}$$

$$s = -2\int \frac{d^3k}{(2\pi)^3}\left[(1-f_k)\ln(1-f_k) + f_k \ln f_k\right] \tag{3.15}$$

where the factor of 2 comes from spin degeneracy and f_k is the Fermi distribution:

$$f_k \equiv \frac{1}{e^{(E_k-\mu)/T}+1} \tag{3.16}$$

with E_k being the single-particle energy

$$E_k = \sqrt{k^2+m^2} \tag{3.17}$$

By substituing Eqs. (3.13)-(3.15) into the pressure equation in Eq. (3.12), we obtain:

$$P = 2T \int \frac{d^3k}{(2\pi)^3} \ln\left[1 + e^{-(E_k-\mu)/T}\right] \tag{3.18}$$

The antiparticle contributions are not necessary here, as they can be neglected due to the large positive chemical potential and low temperature.

We take the limit of $T = 0$, which is a good approximation since the temperature of a compact star is typically in the KeV range and much smaller than the chemical potential and masses of the nucleons. At $T = 0$ the Fermi distribution function becomes a step function [55], $f_k = \Theta(k_F - k)$, where k_F is the Fermi momentum, and the k integrals above are cut off at k_F; explicitly:

$$n = \frac{1}{\pi^2}\int_0^{k_F} dk\, k^2 = \frac{k_F^3}{3\pi^2} \tag{3.19}$$

$$\begin{aligned}\epsilon &= \frac{1}{\pi^2}\int_0^{k_F} dk\, k^2\sqrt{k^2+m^2} \\ &= \frac{1}{8\pi^2}\left[(2k_F^3 + m^2k_F)\sqrt{k_F^2+m^2} - m^4 \ln\left(\frac{k_F + \sqrt{k_F^2+m^2}}{m}\right)\right]\end{aligned} \tag{3.20}$$

$$\begin{aligned}P &= \frac{1}{\pi^2}\int_0^{k_F} dk\, k^2(\mu - \sqrt{k^2+m^2}) \\ &= \frac{1}{24\pi^2}\left[(2k_F^3 - 3m^2k_F)\sqrt{k_F^2+m^2} + 3m^4 \ln\frac{k_F + \sqrt{k_F^2+m^2}}{m}\right]\end{aligned} \tag{3.21}$$

Now, let us consider the total pressure of the star given by summing the contributions of all fermionic particles, which we take as being neutrons (n), protons (p), and electrons:

$$P = \frac{1}{\pi^2}\sum_{i=n,p,e}\int_0^{k_F} dk\, k\left(\mu_i - \sqrt{k^2+m_i^2}\right) \tag{3.22}$$

Here, the individual chemical potentials are not yet fixed. They can be fixed by minimizing the grand potential, or maximizing the pressure, with respect to the individual densities, which ultimately are given in terms of the Fermi momentum. But this minimization by itself is not enough because for the stability of the star one needs charge neutrality and also chemical equilibrium due to the weak interaction.

The minimization condition leads to:

$$\frac{\partial P}{\partial k_{F,i}} = 0 \quad , \quad i = n, p, e \tag{3.23}$$

which implies

$$\mu_i = \sqrt{k_{Fi}^2 + m_i^2} \tag{3.24}$$

Charge neutrality means that that the electron density is equal to the proton density, namely:

$$n_e = n_p \tag{3.25}$$

which implies

$$k_{F,e} = k_{F,p} \tag{3.26}$$

The weak processes

$$n \to p + e + \overline{\nu}_e \tag{3.27}$$

$$p + e \to n + \nu_e \tag{3.28}$$

impose further constraints on the values of the individual Fermi momenta. The first equation above corresponds to neutron β decay whereas the second corresponds proton electron capture. We also assume that the neutrino chemical potential is zero, $\mu_{\nu_e} = 0$, which is a reasonable assumption as their interactions with the the nucleons and electrons is extremely weak so that they leave the system without any further interaction. As a result, we have the constraint:

$$\mu_n = \mu_p + \mu_e \tag{3.29}$$

this implies:

$$\sqrt{k_{F,n}^2 + m_n^2} = \sqrt{k_{F,p}^2 + m_p^2} + \sqrt{k_{F,e}^2 + m_e^2} \tag{3.30}$$

Using Eq (3.26), we can eliminate the electron Fermi momentum and solve the resulting equation to express the proton Fermi momentum in terms of the neutron Fermi momentum

$$k_{F,p}^2 = \frac{(k_{F,n}^2 + m_n^2 - m_e^2)^2 - 2(k_{F,n}^2 + m_n^2 + m_e^2)m_p^2 + m_p^4}{4(k_{F,n}^2 + m_n^2)} \tag{3.31}$$

Let us examine some limiting cases. First, let us assume there is no contribution from protons $k_{F,p} = 0$; then

$$k_{F,n}^2 + m_n^2 = m_p^2 + 2m_p m_e + m_e^2 \Rightarrow k_{F,n}^2 = (m_p + m_e)^2 - m_n^2 < 0 \tag{3.32}$$

The neutron has a slightly larger mass than the combined mass of the electron and proton, $m_p \simeq 938.3$ MeV, $m_n \simeq 939.6$ MeV, $m_e \simeq 0.511$ MeV. This implies that $k_{F,p} = 0$ is impossible and that there must always be at least a small contribution from protons. Instead, let us assume that $k_{F,n} = 0$, which leads to the following scenario:

$$k_{F,p}^2 = \left(\frac{m_n^2 + m_e^2 - m_p^2}{2m_n}\right) - m_e \simeq 1.4\,\mathrm{MeV}^2 \tag{3.33}$$

If the threshold is surpassed, there will be neutrons present, but if threshold is not surpassed, the system will be in β - equilibrium and will consist solely of protons and electrons with the same number density. Assuming a given baryon density $n_B = n_n + n_p$ we can express the neutron Fermi momentum as

$$n_B = \frac{k_{F,p}^3}{3\pi^2} + \frac{k_{F,n}^3}{3\pi^2} \Rightarrow k_{F,n} = (3\pi^2 n_B - k_{F,p}^3)^{1/3} \tag{3.34}$$

In the case where we can neglect all masses, i.e, the ultra-relativistic limit, Eq (3.31), we can be expressed as follows:

$$k_{F,p}^2 = \frac{k_{F,n}^4}{4k_{F,n}^2} \Rightarrow k_{F,p} = \frac{k_{F,n}}{2} \tag{3.35}$$

and thus

$$n_p = \frac{n_B}{9} \tag{3.36}$$

Let us examine the scenario of pure neutron matter under the assumption of the nonrelativistc limit, $m_n >> k_{F,n}$. In the case, the energy density Eq. (3.20) and pressure (3.21) simplify to

$$\begin{aligned} \epsilon &\simeq \frac{m_n^4}{3\pi^2}\left[\frac{k_{F,n}^3}{m_n^3} + \mathcal{O}\left(\frac{k_{F,n}^5}{m_n^5}\right)\right] \\ P &\simeq \frac{m_n^4}{15\pi^2}\left[\frac{k_{F,n}^5}{m_n^5} + \mathcal{O}\left(\frac{k_{F,n}^7}{m_n^7}\right)\right] \end{aligned} \tag{3.37}$$

which can be easily proved by expanding the square-root and logarithm function in porwers of $k_{F,n}/m_n$. Then, we obtain:

$$\epsilon = \frac{k_{F,n}^3}{3\pi^2} m_n \Rightarrow k_{F,n} = \left(\frac{3\pi^2\epsilon}{m_n}\right)^{1/3}$$

and so

$$P \simeq \frac{m_n^4}{15\pi^2}\left[\left(\frac{3\pi^2\epsilon}{m_n^4}\right)^{5/3}\right] \simeq \left(\frac{3\pi^2}{m_n}\right)^{5/3} \frac{\epsilon^{5/3}}{15 m_n \pi^2} \tag{3.38}$$

One can derivate the mass-radius relation of the state by substituting the equation of state into TOV equation. A common type of equation of state used to model the behavior of dense matter is known as the polytropic equation of state, which has a general from of

$$P(\epsilon) = k\epsilon^{\gamma} \tag{3.39}$$

Expressing the equations in the Newtonian form, as given in Eqs (3.9) leads to the following

$$\begin{aligned} \frac{dm}{dr} &= \frac{4\pi}{k^{1/\gamma}} r^2 P^{1/\gamma}(r) \\ \frac{dP}{dr} &= -\frac{G}{k^{1/\gamma}} \frac{P^{1/\gamma}(r) m(r)}{r^2} \end{aligned} \tag{3.40}$$

3.2 Properties of symmetric nuclear matter

Before discussing an interacting model, let us discuss briefly the properties of symmetric nuclear matter. The properties of nuclear matter are inferred from the experimentally observed properties of finite nuclei [54]. In this study, the values of nuclear matter properties provided in Ref. [54] will be considered as the observed values.

3.2.1 Saturation density

Nuclear matter is a saturated system due to the characteristics of strong interaction. The short-range strong nuclear interaction is the dominant force between nucleons. It is primarily attractive, necessary for the formation of stable nuclei, but becomes repulsive at short distances ($\leq 0.4\ fm$). As the strong force only operates over short distances, the interaction is limited to the closestneighbors in a dense system. Consequently, at a certain density, the central density of the system will not increase further, even with the addition of more nucleons. This density is referred to as saturation density. At saturation density, the system's pressure is zero, and it will remain in this state if left undisturbed [49].

The density of saturated nuclear matter given as 0.153 fm^{-3} in Ref. [54]

3.2.2 Binding energy

In broad terms, the binding energy of a system represents the energy consumed or required for its formation. In the case of a stable system, this energy is negative, signifying that energy has been released into the environment during formation, thus placing the system in a lower energy state compared to the sum of its individual components.

At saturation density, the system's binding energy reaches its minimum, indicating that the system is at its most stable state (lowest energy) compared to other densities. The binding energy of nuclear matter is reported as -16.3 MeV/nucleon in Ref. [54].

3.2.3 Compression modulus

The compression modulus defines the curvature of the equation of state at saturation [49] and is associated with the high density behavior of the equation of state. If the energy density increases rapidly with pressure, the equation of state is referred to as stiff. In contrast, with a soft equation of state, the energy density increases more gradually with increasing pressure [49]. The compression modulus, K, is defined as

$$K \equiv k_F^2 \frac{\partial^2(\epsilon/n_B)}{\partial {k_F}^2} \tag{3.41}$$

The estimated value of K was approximately 250 MeV (with some uncertainty) [49]. We will delve into the details of this further in the next Section.

3.3 Walecka Model

In 1974, JD Walecka introduced a relativistic quantum field theory to describe nuclei and nuclear matter through meson exchange [16], commonly known as the Walecka model or quantum hadrodynamics (QHD). Given the complexity of nuclei and nuclear matter, multiple models have been developed afterward. Each model relies on experimental data to guide its formulation. In the case of QHD, the unknown parameters are the meson-nucleon coupling constants. These constants are determined fitting the model's calculated properties of nuclei and nuclear matter (as discussed in the section) with experimentally observed (or inferred) values. Over the years, different sets of parameters for QHD have emerged as researchers have adjusted them to match various other observed properties of nuclei and/or nuclear matter. These parameter sets may differ significantly by incorporating additional meson fields, varying couplings between different fields, or recalculated coupling constant values.

This model in its simplest form describes interactions between nucleons through the exchange of scalar σ and vector ω mesons. Pions, are the lightest mesons , for this reason are not included in the Walecka model. This low mass means that pions mediate long-range interactions, which are less significant in the mean-field approximation used by the Walecka model. Its Lagrangian is given by the sum of free nucleon $\mathcal{L}_N$ and meson $\mathcal{L}_{\sigma,\omega}$ Lagrangians and meson-nucleon interaction $\mathcal{L}_I$ Lagrangian:

$$\mathcal{L} = \mathcal{L}_N + \mathcal{L}_{\sigma,\omega} + \mathcal{L}_I \tag{3.42}$$

We start writing each of these Lagrangian in Mickowski space. The free nucleon Lagrangian is given by

$$\mathcal{L}_N = \overline{\psi}\left(i\gamma^\mu \partial_\mu - m_N\right)\psi \tag{3.43}$$

where ψ is the nucleon isospin doublet

$$\psi = \begin{pmatrix} \psi_n \\ \psi_p \end{pmatrix} \tag{3.44}$$

with ψ_n and ψ_p being respectively the neutron and proton Dirac spinor fields, and m_N is the nucleon mass matrix

$$m_N = \begin{pmatrix} m_n & 0 \\ 0 & m_p \end{pmatrix} \tag{3.45}$$

As usual, $\overline{\psi} \equiv \psi^\dagger \gamma^0$. The $\mathcal{L}_{\sigma,\omega}$ free mesonic Lagrangian is given by

$$\mathcal{L}_{\sigma,\omega} = \frac{1}{2}\left(\partial_\mu \sigma \partial^\mu \sigma - m_\sigma^2 \sigma^2\right) - \frac{1}{4}\omega_{\mu\nu}\omega^{\mu\nu} + \frac{1}{2} m_\omega^2 \omega_\mu \omega^\mu \tag{3.46}$$

with $\omega_{\mu\nu} \equiv \partial_\mu \omega_\nu - \partial_\nu \omega_\mu$. The $\mathcal{L}_I$ interaction Lagrangian is given by Yukawa nucleon-meson interactions:

$$\mathcal{L}_I = g_\sigma \overline{\psi} \sigma \psi + g_\omega \overline{\psi} \gamma^\mu \omega_\mu \psi \tag{3.47}$$

To obtain the equation of state, we must compute the partition function corresponding to the model for a given temperature $T = 1/\beta$ and neutron and proton chemical potentials μ_n and μ_p:

$$Z = \text{Tr} \exp \left[-\beta \left(\hat{H} - \sum_{i=p,n} \mu_i \hat{N}_i \right) \right] \tag{3.48}$$

where $\hat{H}$ is the Hamiltonian operator corresponding to the Lagrangian L and $\hat{N}_i = \overline{\psi}_i \gamma^0 \psi_i = \psi_i^\dagger \psi_i,\ i = n, p$ are the neutron and proton number operators. The trace can be expressed in terms of a functional integral in the traditional way [55], namely:

$$Z = \int \mathcal{D}\overline{\psi} \mathcal{D}\psi \mathcal{D}\sigma \mathcal{D}\omega \ \exp \left[\int_X \left(\mathcal{L}_E - \overline{\psi} \gamma_0 \mu \psi \right) \right] \tag{3.49}$$

where $\mathcal{L}_E$ is the Euclidean counterpart of the Minkowski space $\mathcal{L}$, and we used the shorthand notation

$$\int_X \equiv \int_0^\beta d\tau \int d^3x \tag{3.50}$$

with μ being the chemical potential matrix

$$\mu = \begin{pmatrix} \mu_n & 0 \\ 0 & \mu_p \end{pmatrix} = \begin{pmatrix} \mu_B + \mu_I & 0 \\ 0 & \mu_B - \mu_I \end{pmatrix} \tag{3.51}$$

where $\mu_B = (\mu_n + \mu_p)/$ and $\mu_I = (\mu_n - \mu_p)/2$ are the baryon and isospin chemical potentials, respectively. The meson fields $\sigma(\tau, \mathbf{x})$ and $\omega(\tau, \mathbf{x})$ are periodic in the variable τ and the nucleon field is antiperiodic, with period $\beta = 1/T$ (recall we are using units $\hbar = c = k = 1$):

$$\sigma(\tau, \mathbf{x}) = \sigma(\tau + \beta, \mathbf{x}) \qquad \text{and} \qquad \omega_\mu(\tau, \mathbf{x}) = \omega_\mu(\tau + \beta, \mathbf{x}) \tag{3.52}$$

$$\psi(\tau, \mathbf{x}) = -\psi(\tau, \mathbf{x}) \tag{3.53}$$

We decompose each meson fields as a sum of its expectation value (mean field) plus a flutuation:

$$\sigma = \overline{\sigma} + \sigma' \tag{3.54}$$

$$\omega_\mu = \overline{\omega}_0\, \delta_{0\mu} + \omega'_\mu \tag{3.55}$$

The mean field of the vector field has only the zero-th component due to rotational invariance of nuclear matter and pure-neutron matter. For finite nuclei that are not spherically symmetric, the spatial components of the vector mean field also contribute. We will employ the traditional mean field approximation, a.k.a. Hartree approximation. This approximation consists in neglecting the fluctuations σ' and ω'_μ. As a consequence, the mesonic fields, which were variables in Lagrangian (3.42) and integrated in the functional integral defining the partition function, can now be replaced by their expected values. As a result, the partition function is then given by:

$$Z = e^{\frac{V}{T}\left(-\frac{1}{2}m_\sigma^2\overline{\sigma}^2+\frac{1}{2}m_\omega^2\overline{\omega}_0^2\right)} \int \mathcal{D}\overline{\psi}\mathcal{D}\psi\ \exp\left[\int_{\mathbf{x}} \overline{\psi}(i\gamma^\mu\partial_\mu - m_N^* + \mu^*\gamma_0)\psi\right] \tag{3.56}$$

where V is the volume, $\gamma^\mu\partial_\mu = -\gamma^0\partial_\tau - i\boldsymbol{\gamma}\cdot\boldsymbol{\nabla}$, and

$$m_N^* \equiv m_N - g_\sigma\overline{\sigma} \tag{3.57}$$

$$\mu^* \equiv \mu - g_\omega\overline{\omega}_0 \tag{3.58}$$

Clearly, the sole effect of meson Yukawa interactions in this mean field approximation is giving an effective mass to the nucleon m_N^* and an effective chemical potential μ^*.

To integrate the remaining functional integrals over the nucleon fields, we use Fourier transform

$$\psi(X) = \frac{1}{\sqrt{V}}\sum_K e^{-iK\cdot X}\psi(K) \quad , \quad \overline{\psi}(X) = \frac{1}{\sqrt{V}}\sum_K e^{iK\cdot X}\overline{\psi}(K) \tag{3.59}$$

being $K = (-i\omega_n, \mathbf{k})$, $X = (-i\tau, \mathbf{x})$, and $K\cdot X = k_0x_0 - \mathbf{k}\cdot\mathbf{x} = -(\omega_n\tau + \mathbf{k}\cdot\mathbf{x})$, where ω_n are the fermionic Matsubara frequencies $\omega_n = (2n+1)\pi T$, which follow from the anti-periodicity of the nucleon field. In terms of the Fourier-transformed fields, the action becomes diagonal:

$$Z = e^{\frac{V}{T}\left(-\frac{1}{2}m_\sigma^2\overline{\sigma}^2+\frac{1}{2}m_\omega^2\overline{\omega}_0^2\right)} \int \mathcal{D}\psi^\dagger\mathcal{D}\psi\, \exp\left[-\sum_K \psi^\dagger(K)\frac{G^{-1}(K)}{T}\psi(K)\right] \tag{3.60}$$

where

$$G^{-1}(K) = -\gamma^\mu K_\mu - \gamma_0 \mu^* + m_N \tag{3.61}$$

is the inverse nucleon propagator. The the functional integral can be readily integrated, leading to the following result for the partition function:

$$Z = e^{\frac{V}{T}\left(-\frac{1}{2}m_\sigma^2\overline{\sigma}^2 + \frac{1}{2}m_\omega^2\overline{\omega}_0^2\right)} \det\left[\frac{G^{-1}(K)}{T}\right] \tag{3.62}$$

The computation of the determinant is straightforward: one computes it for a given value K and the make the product of each of them. Since we want $\ln Z$, the log of the product over K turns into a sum over K. Performing the Matsubara sum and considering the thermodynamic limit, we obtain

$$\begin{aligned}\ln Z = &\frac{V}{T}\left(-\frac{1}{2}m_\sigma^2\overline{\sigma}^2 + \frac{1}{2}m_\omega^2\overline{\omega}_0^2\right) \\ &+ 4V\int \frac{d^3\mathbf{k}}{(2\pi)^3}\left[\frac{E_k}{T} + \ln\left(1 + e^{-(E_k-\mu^*)/T}\right) + \ln\left(1 + e^{-(E_k+\mu^*)/T}\right)\right]\end{aligned} \tag{3.63}$$

where

$$E_k = \sqrt{k^2 + (m_N^*)^2} \tag{3.64}$$

is the single-nucleon energy. Details of the above derivations are given in **Appendix** A.3.

The pressure is given by

$$P = \frac{T}{V}\ln Z = -\frac{1}{2}m_\sigma^2\overline{\sigma}^2 + \frac{1}{2}m_\omega^2\overline{\omega}_0^2 + P_N \tag{3.65}$$

with

$$P_N \equiv 4V\int \frac{d^3\mathbf{k}}{(2\pi)^3}\left[\ln\left(1 + e^{-(E_k-\mu^*)/T}\right) + \ln\left(1 + e^{-(E_k+\mu^*)/T}\right)\right] \tag{3.66}$$

By maximizing the pressure to determine the meson condensates, from Eq. (3.65), we have

$$0 = \frac{\partial P}{\partial\overline{\sigma}} = -m_\sigma^2\overline{\sigma} + \frac{\partial P_N}{\partial\overline{\sigma}}$$

but we can write

$$\frac{\partial P_N}{\partial\overline{\sigma}} = \frac{\partial P_N}{\partial m^*}\underbrace{\frac{\partial m^*}{\partial\overline{\sigma}}}_{-g_\sigma}$$

so that

$$0 = \frac{\partial P}{\partial \overline{\sigma}} = -m_\sigma^2 \overline{\sigma} - g_\sigma \frac{\partial P_N}{\partial m_N^*} \tag{3.67}$$

$$0 = \frac{\partial P}{\partial \overline{\omega}_0} = m_\omega^2 \overline{\omega}_0 - g_\omega \frac{\partial P_N}{\partial \mu^*} \tag{3.68}$$

We can further rewrite the equations above in terms of baryon and scalar densities. For that, we have to compute them first:

$$\begin{aligned} n_B &= \langle \psi^\dagger \psi \rangle = \frac{\partial P_N}{\partial \mu} = \frac{\partial P_N}{\partial \mu^*} \\ &= 4 \sum_{e=\pm} e \int \frac{d^3\mathbf{k}}{(2\pi)^3} \frac{1}{e^{(E_k - e\mu^*)/T} + 1} \end{aligned} \tag{3.69}$$

and

$$\begin{aligned} n_s &= \langle \overline{\psi} \psi \rangle = -\frac{\partial P_N}{\partial m_N^*} \\ &= 4 \sum_{e=\pm} \int \frac{d^3\mathbf{k}}{(2\pi)^3} \frac{m_N^*}{E_k} \frac{1}{1 + e^{(E_k - e\mu^*)}} \end{aligned} \tag{3.70}$$

Fianally, we obtain

$$\overline{\sigma} = \frac{g_\sigma}{m_\sigma^2} n_s \tag{3.71}$$

$$\overline{\omega}_0 = \frac{g_\omega}{m_\omega^2} n_B \tag{3.72}$$

Substituting Eq. (3.71) into Eq. (3.57), we have

$$m_N^* = m_N - \frac{g_\sigma^2}{m_\sigma^2} n_s \tag{3.73}$$

Since the temperature here in our context are of the order of 10 MeV, so we can consider the temperature to be zero. In this sense, the Fermi distribution becomes a step function. It is worth recalling that the chemical potential related to the baryon number n_B is μ, not μ^*. Therefore, the pressure at zero temperature is given by $P = -\epsilon + \mu n_B$ and knowing that P_N can be written as $-\epsilon_0 + \mu^* n_B$, we have:

$$\epsilon_0 = \frac{1}{4\pi} \left[(2k_F^3 + (m_N^*)^2 k_F) E_F^* - (m_N^*)^4 \ln \left(\frac{k_F + E_F^*}{m_N^*} \right) \right] \tag{3.74}$$

given by Eq. (3.20) with the difference that we account for two additional degrees of freedom.

$$\begin{aligned} P &= \frac{1}{2}\frac{g_\omega^2}{m_\omega^2}n_B^2 - \frac{1}{2}\frac{g_\sigma^2}{m_\sigma^2}n_s^2 \\ &+\frac{1}{4\pi}\left[\left(\frac{2}{3}k_F^3-(m_N^*)^2k_F\right)E_F^*+(m_N^*)^2\ln\left(\frac{k_F+E_F^*}{m_N^*}\right)\right] \end{aligned} \tag{3.75}$$

and we can determine ϵ as follows:

$$P = -\epsilon_0 + \mu^* n_B + \frac{1}{2}\frac{g_\omega^2}{m_\omega^2}n_B^2 - \frac{1}{2}\frac{g_\sigma^2}{m_\sigma^2}n_s^2 \tag{3.76}$$

but $\mu^* = \mu - g_\omega^2 \overline{\omega}_0$, therefore:

$$P = -\left(\epsilon_0 + \frac{1}{2}\frac{g_\omega^2}{m_\omega^2}n_B^2 + \frac{1}{2}\frac{g_\sigma^2}{m_\sigma^2}n_s^2\right) + \mu n_B \tag{3.77}$$

and

$$\begin{aligned} \epsilon &= \frac{1}{2}\frac{g_\omega^2}{m_\omega^2}n_B^2 + \frac{1}{2}\frac{g_\sigma^2}{m_\sigma^2}n_s^2 \\ &+\frac{1}{4\pi^2}\left[(2k_F^3+(m_N^*)^2k_F)E_F^*-(m_N^*)^4\ln\left(\frac{k_F+E_F^*}{m_N^*}\right)\right] \end{aligned} \tag{3.78}$$

where $\mu^* = E^* = \sqrt{k_F^2 + (m_N^*)^2}$. The baryonic and scalar densities at zero temperature are respectively

$$n_B = \frac{2k_F^3}{3\pi^2} \tag{3.79}$$

$$n_s = \frac{m_N^*}{\pi^2}\left[k_F E_F^* - (m_N^*)^2 \ln\left(\frac{k_F+E_F^*}{m_N^*}\right)\right] \tag{3.80}$$

We see that the Equations (3.75) and (3.78) already define the equation of state that can be determined numerically. For an analytical discussion, let us consider small ($k_F \to 0$) and large ($k_F \to \infty$) densities. For small density, we have

$$n_s \simeq \frac{2k_F^3}{3\pi^2} = n_B \tag{3.81}$$

where we neglect terms of $\mathcal{O}\left(\frac{k_F^5}{(m_N^*)^5}\right)$ and higher. Neglecting terms of the order of

$k_F^3/m_\sigma^2 << m_N$ as well, we can conclude from Eq. (3.73) that

$$m_N^* \simeq m_N \tag{3.82}$$

thus

$$P \simeq \frac{2k_F^5}{15\pi^2 m_N} \quad , \quad \epsilon \simeq \frac{2m_N k_F^3}{3\pi^2} \tag{3.83}$$

Therefore, in this small-density approximation, we observe that the pressure and energy density Eq. (3.83) are dominated by nucleonic pressure and reproduce the same results for non-interacting (See Eq. 3.38) case since the effects of interaction are only present in the modification of μ and m_N. which, of course were neglected in this approximation resulting in the equation of the state having the form $P \propto \epsilon^{5/3}$.

Now, for large k_F, we obtain

$$n_s \simeq \frac{m_N^* k_F^2}{\pi^2} \tag{3.84}$$

and then

$$m_N^* \simeq \frac{m_N}{1 + \frac{g_\sigma^2 k_F^2}{m_\sigma^2 \pi^2}} \tag{3.85}$$

With Eq. (3.85), it becomes evident that the effective nucleon mass m_N^* goes zero for high densities. Solving Eq. (3.73) and Eq. (3.85) numerically, we obtain the figure 3.1.

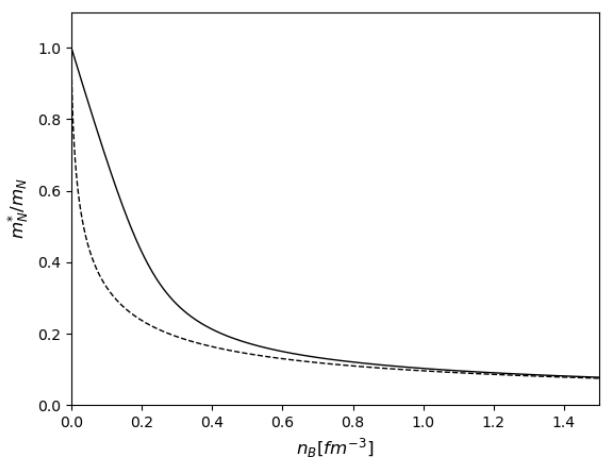

Figure 3.1: The Eq. (3.73) numerically solved for general values of k_F (solid line) and Eq. (3.85) for the high approximation density (dashed line).

In this approximation, we can see that both the nucleonic pressure and the pressure the scalar meson are proportional to k^4. Therefore, the total pressure in this case is dominated by the pressure coming from the contribution of the vector meson which is proportional to k^6.

$$P \simeq \epsilon \simeq \frac{1}{2} \frac{g_\omega^2}{m_\omega^2} n_B \tag{3.86}$$

To use this quantitatively, we must determine the values of the coupling constants. For this purpose, they need to reproduce the following values

$$n_0 = 0.153 \mathrm{fm}^{-3} \quad , \quad E_0 \equiv \left(\frac{\epsilon}{n_B} - m_N \right)_{n_B = n_0} \tag{3.87}$$

where n_0 is the saturation density and E_0 is the binding energy per nucleon at saturation with these values. The coupling values $g_\omega^2/4\pi = 14.717$ and $g_\sigma^2/4\pi = 9.537$ reproduce those values. The following figure shows the binding energy per nucleon predicted by the model.

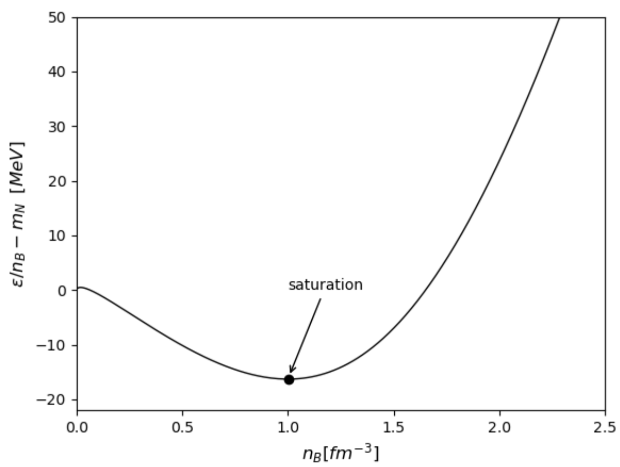

Figure 3.2: The binding energy per nucleon at zero temperature in the Walecka model computed as a function of baryon density by evaluating the energy density with the density-modified nucleon mass.

It is evident from Fig. 3.2 that there is a finite density n_0 at which the binding energy is minimum. In this case, if you add nucleons to a very large nucleus, the density will remain approximately constant due to the fact that the nucleons have a preferred distance between them at which the energy is minimized. We can also see in the figure that the minimum energy divides the graph into a stable region (with positive pressure) and an unstable region (with negative pressure). This pressure can be represented by the simple thermodynamic relation $P = -\partial E/\partial V$, with $E = \epsilon V$ being the energy and V the volume. Therefore, this implies

$$P = n_B^2 = \frac{\partial(\epsilon/n_B)}{\partial n_B} \tag{3.88}$$

From this result, we see that indeed the minimum of ϵ/n_B corresponds to zero pressure in the system. It is worth noting that as the binding energy per baryon decreases while the baryon number increases, we observe that the pressure becomes negative.

Taking this case into context of compact stars, this self-boundedness behavior (i.e, it is stable at zero pressure) of nuclear matter may imply the existence of nuclear matter on the surface of the star, where the pressure is zero. However, in the interior of the star, we encounter gravitational pressure that compresses the matter to densities higher than the saturation density n_0. It is evident in the figure that the compressed matter has its own positive pressure that counterbalances the gravitational pressure. It is for this reason that the high-density part in the figure has important astrophysical applications. We will see later on that the simple Walecka Model we studied here does not provide reliable results for densities higher than the saturation density, and there exists a peculiar way to improve the model.

We can observe from the previous figure that the extrapolated binding energy at high densities increases substantially. The model fails to accurately calculate the incompressibility of nuclear matter, defined in Eq. (3.41). This quantity, as discussed in the previous section, measures the stiffness of nuclear matter and its values are already well established experimentally. To highlight the magnitude of this discrepancy, let us first consider the thermodynamic definition of compressibility χ to see if higher values of K correspond to a stiffer matter

$$\frac{1}{\chi} = n_B \frac{\partial P}{\partial n_B} = n_B^2 \frac{\partial^2 \epsilon}{\partial {n_B}^2} \tag{3.89}$$

Referring to Eq. (3.41), we can observe that

$$K = k_F^2 \frac{\partial^2(\epsilon/n_B)}{\partial {n_B}^2} \left(\frac{\partial n_B}{\partial k_F}\right)^2 = 9 n_B^2 \frac{\partial^2(\epsilon/n_B)}{\partial {n_B}^2} \tag{3.90}$$

thus,

$$
\begin{aligned}
K = 9n_B^2 \frac{\partial^2(\epsilon/n_B)}{\partial {n_B}^2} &= 9n_B \frac{\partial^2 \epsilon}{\partial {n_B}^2} - 18\frac{\partial \epsilon}{\partial n_B} + \frac{18\epsilon}{n_B} \\
&= 9n_B \frac{\partial^2 \epsilon}{\partial {n_B}^2} + 18\left(\frac{\epsilon}{n_B} - \frac{\partial \epsilon}{\partial n_B}\right)
\end{aligned} \tag{3.91}
$$

where

$$
0 = \frac{\partial(\epsilon/n_B)}{\partial n_B}\bigg|_{n_B=n_0} = -\frac{1}{n_B}\left(\frac{\epsilon}{n_B} - \frac{\partial \epsilon}{\partial n_B}\right) \tag{3.92}
$$

has been used. From this, it follows that:

$$
K = \frac{9}{n_B} n_B^2 \frac{\partial^2 \epsilon}{\partial {n_B}^2} = \frac{9}{n_B \chi} \implies \frac{1}{\chi} = \frac{n_0 K}{9} \tag{3.93}
$$

Consequently, a significant compressibility χ is synonymous with a minimal incompressibility K, as it should be.

Calculating incompressibility in this model results in a value of $K \simeq 560$ MeV, which is more than double the experimentally inferred value for a large nucleus. Therefore, the fact that the calculated value is significantly higher than the experimental value indicates that this will involve discrepancies between the model predictions and the observational data. We can also compare the mass of the nucleon, which can be experimentally mass and the model prediction of this model. This comparison between the experimental mass and the model prediction is another important test to assess the consistency of the model with observations.

3.3.1 Scalar-Meson Self Interactions

In order to make the Walecka model more consistent with experimental data, scalar-meson cubic and quartic self-interactions interactions are included in the model Lagrangian [54], namely:

$$
\mathcal{L}_{I,\sigma} = -\frac{b}{3} m_N (g_\sigma \sigma)^3 - \frac{c}{4} (g_\sigma \sigma)^4 \tag{3.94}
$$

The resulting model is also called nonlinear Walecka model (NLWM). These meson self-interactions induce multinucleon forces, as in the mean field approximation, each $\overline{\sigma}$ field is sourced by the scalar condensate, which is given in terms of $\overline{\psi}\psi$.

In addition to the empirical necessity of incorporating the self-interaction terms into the Walecka model to reproduce experimental data, there is also a theoretical rationale for their inclusion. This rationale is linked to the model's renormalization process. By introducing the self-interaction terms, two new dimensionless constants b and c are introduced. These constants, along with the g_σ and g_ω couplings, can be adjusted to match four experimental values: The saturation density and binding energy (as described in Eq. (3.87)), incompressibility and Landau mass

$$K \simeq 250 \text{ MeV} \quad , \quad m_L = 0.83 m_N \tag{3.95}$$

where the Landau mass is defined as

$$m_L = \frac{k_F}{v_F} \tag{3.96}$$

with v_F being the Fermi velocity:

$$v_F = \frac{\partial E_k}{\partial k}|_{k=k_F} \tag{3.97}$$

It is worth noting that the Landau mass is experimentally easier to measure compared to the mass parameter m^*, as it represents the effective mass for fermions at the Fermi surface where low-energy excitations are concentrated.

So, including the mean field approximation and following the previously established procedures, adding the self-interaction terms to the scalar field, the pressure becomes

$$P = -\frac{1}{2}m_\sigma^2\overline{\sigma}^2 - \frac{b}{3}m_N(g_\sigma\overline{\sigma})^3 - \frac{c}{4}(g_\sigma\overline{\sigma})^4 + \frac{1}{2}m_\omega^2\overline{\omega}_0^2 + P_N \tag{3.98}$$

$$0 = \frac{\partial P}{\partial \overline{\sigma}} = -m_\sigma^2\overline{\sigma} - b m_N g_\sigma^3\overline{\sigma}^2 - c g_\sigma^4\overline{\sigma}^3 + g_\sigma n_s$$

$$\Rightarrow \overline{\sigma} = \frac{1}{m_\sigma^2}(-b m_N g_\sigma^3\overline{\sigma}^2 - c g_\sigma^4\overline{\sigma}^3 + g_\sigma n_s)$$

On the other hand, we that $\overline{\sigma}$ is related to an effective nucleon mass as

$$\overline{\sigma} = \frac{1}{g_\sigma}(m_N - m_N^*)$$

Therefore

$$\overline{\sigma} = \frac{1}{m_\sigma^2}[-b m_N g_\sigma(m_N - m_N^*)^2 - c g_\sigma(m_N - m_N^*)^3 + g_\sigma n_s] \tag{3.99}$$

Substituting this into (3.67), we obtain

$$m_N^* = m_N - \frac{g_\sigma^2}{m_\sigma^2} n_s + \frac{g_\sigma^2}{m_\sigma^2}\left[b m_N (m_N - m_N^*)^2 + c(m_N - m_N^*) \right] \tag{3.100}$$

In order to obtain the binding energy per nucleon as a function of baryon density, let us calculate the energy density for this case. In the same way as was done in Eq. 3.77, we have:

$$\begin{aligned} P &= \epsilon_0 + \mu^* n_B - \frac{1}{2} m_\sigma^2 \overline{\sigma}^2 - \frac{b}{3} m_N (g_\sigma \overline{\sigma})^3 - \frac{c}{4} (g_\sigma \overline{\sigma})^4 + \frac{1}{2} m_\omega^2 \overline{\omega}_0^2 \\ P &= -\left(\epsilon_0 + \frac{1}{2} \frac{g_\omega^2}{m_\omega^2} n_B^2 + \frac{1}{2} m_\sigma^2 \sigma^2 + \frac{b}{3} m_N (g_\sigma \overline{\sigma})^3 + \frac{c}{4} (g_\sigma \overline{\sigma})^4 \right) \end{aligned} \tag{3.101}$$

so,

$$\begin{aligned} \epsilon &= \frac{1}{2} \frac{g_\omega^2}{m_\omega^2} n_B^2 + \frac{1}{2} m_\sigma^2 \sigma^2 + \frac{b}{3} m_N (g_\sigma \overline{\sigma})^3 + \frac{c}{4} (g_\sigma \overline{\sigma})^4 \\ &\quad + \frac{1}{4\pi^2} \left[(2k_F^3 + (m_N^*)^2 k_F) E_F^* - (m_N^*)^4 \ln \left(\frac{k_F + E_F^*}{m_N^*} \right) \right] \end{aligned} \tag{3.102}$$

With the aim of adjusting the free parameters, we should select the values $g_\sigma^2/(4\pi) = 6.003$, $g_\omega^2/(4\pi) = 5.948$, $b = 7.950 \cdot 10^{-3}$, and $c = 6.952 \cdot 10^{-4}$. The results for the binding energy are shown in Fig. 3.3. It becomes apparent that the behavior of the result for higher densities, as depicted in this figure, has undergone significant changes compared to the case without scalar self-interactions. In this scenario, the lower incompressibility value is associated with a smoother equation of state at high densities.

3.3.2 Results for the Mass-Radius Relation

Now, we present the results of the analysis of the mass-radius relation for neutron stars using the equation of state of the traditional Walecka model and the Walecka model including the scalar-meson self-interactions (NLWM). Given the simplicity of the models, one does not expect that they will provide a precise description of a neutron star. But these models do provide insight into such a complex system and are extremely helpful in guiding our intuition. As such, we do not enforce β-equilibrium. Therefore, one should keep in mind the predictions are not for a real star. We integrate our EoS into a program that solves the Tolman-Oppenheimer-Volkoff (TOV) equation, allowing for a numerical analysis of the

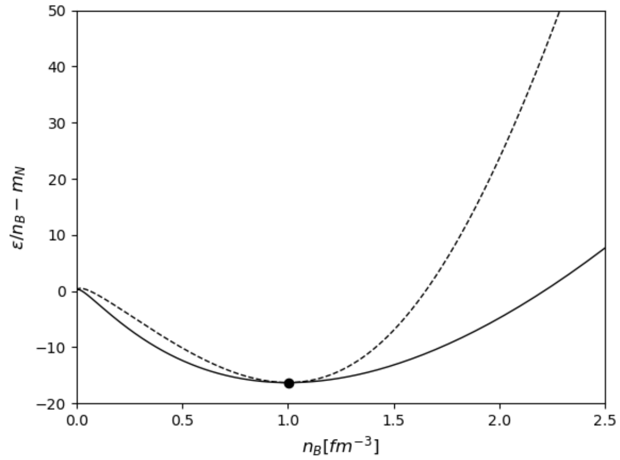

Figure 3.3: The binding energy per nucleon at zero temperature in the Walecka model including cubic and quartic scalar self-interactions (solid line).

mass-radius relation. Solving the Eq. (3.10) for the equation of state expressed by the equations (3.78) and (3.75), we obtain the following result:

$M_{max}[M_0]$	2.98
$R_{max}(Km)$	13.848

It is interesting to observe that the model describes well real neutron stars, despite of the limitations of the calculation. It is noted that the typical radius of these stars ranges around 12 kilometers, while their masses usually fall between 1.0 $M_\odot$ and 2.0 $M_\odot$. However, there is nothing preventing the existence of neutron stars with even larger masses. The maximum mass estimate in this model is significant, surpassing the mass of the most massive neutron star ever recorded, which is approximately 2.35 ± 0.17 $M_\odot$ [56], and remains below the theoretical maximum limit of about 3.2 solar masses for neutron stars. Figure (3.4), on the left panel, depicts the mass-radius relation for neutron stars modeled by the Walecka model.

Now, solving the TOV equation for the equation of state of NLWM given by Eqs. (3.101) and (3.102), we obtain

$M_{max}[M_0]$	2.042
$R_{max}(Km)$	10.410

This ends up not being such a good result because, as previously mentioned, the most massive neutron star measured to date, PSR J0952-0607, has 2.35 ± 0.17 $M_\odot$ [56]. In Fig. (3.4), on the right panel, we plot the mass-radius relation for this model.

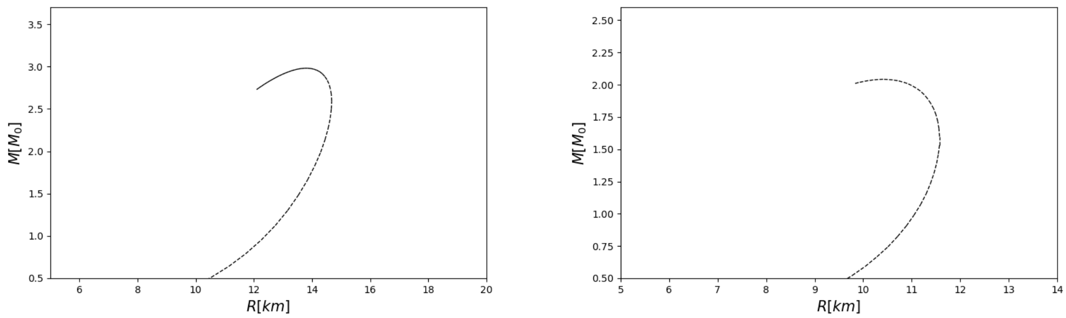

Figure 3.4: **Left panel:** M-R relation for Walecka Model. **Right panel:**M-R relation for Walecka Model with scalar-meson self interactions (NLWM).

Chapter 4

Quark exchange in nuclear and pure-neutron matter

For point-like nucleons, the Pauli exclusion principle operates at the nucleon level. As density increases, the nucleon get closer together and the quarks that make up nucleons start to reveal their internal structure as the nucleon wave functions overlap. Then, the Pauli principle operates at the quark level. This changes the single-particle nature of the mean-field description of nuclear matter and pure neutron matter we have been discussing [21, 22]. This means that quarks from different nucleons contribute even for single-particle (nucleon or quark) matrix elements because the wave functions of the two different nucleons overlap. We elaborate on this point.

Suppose that one wants to compute the expectation value of the quark kinetic energy operator, which is a single-particle operator, in a state of two nucleons. At the quark level, one can write this operator as (her and in the following equations, a sum over repeated indices is implied)

$$\hat{K} = K(\mu)\, \hat{q}^{\dagger}_{\mu}\hat{q}_{\mu} \tag{4.1}$$

where $\hat{q}^{\dagger}_{\mu}$ and $\hat{q}_{\mu}$ are quark creation and annihilation operators, μ collects all quantum numbers of the quarks, namely color, flavor, spin, and momentum. For nonrelativistic quarks, we have $K(\mu) = \mathbf{p}^2/2m$ and for relativistic quarks $K(\mu) = (\mathbf{p}^2 + m^2)^{1/2}$, where m is the quark mass. The quark creation and annihilation operators satisfy canonical anticommutation relations:

$$\{\hat{q}_{\mu}, \hat{q}^{\dagger}_{\nu}\} = \delta_{\mu\nu}, \qquad \{\hat{q}_{\mu}, \hat{q}_{\nu}\} = \{\hat{q}^{\dagger}_{\mu}, \hat{q}^{\dagger}_{\nu}\} = 0 \tag{4.2}$$

Let us write the two-nucleon state as

$$|nn'\rangle = \hat{B}^{\dagger}_{n}\hat{B}^{\dagger}_{n'}|0\rangle \tag{4.3}$$

where $\hat{B}_n^\dagger$ is a nucleon creation operator, n indicates all quantum numbers of the nucleon: isospin (neutron or proton), spin, center-of-mass momentum. In a constituent-quark model, $\hat{B}_n^\dagger$ is given by the product of three quark creation operators coupled together by a three-quark wave function $\Psi_n^{\mu_1\mu_2\mu_3}$, which is a color singlet and gives the quantum number n:

$$B_n^\dagger = \frac{1}{\sqrt{3!}} \Psi_n^{\mu_1\mu_2\mu_3} \, \hat{q}_{\mu_1}^\dagger \hat{q}_{\mu_2}^\dagger \hat{q}_{\mu_3}^\dagger \tag{4.4}$$

The factor $1/\sqrt{3!}$ is introduced to obtain a simple normalization condition for the $\Psi_n^{\mu_1\mu_2\mu_3}$; namely, using the anticommutation relations in Eq. (4.2), one obtains:

$$\langle n|n'\rangle = \Psi_n^{*\mu_1\mu_2\mu_3} \Psi_{n'}^{\mu_1\mu_2\mu_3} = \delta_{nn'} \tag{4.5}$$

In addition, using Eqs. (4.2) and (4.5), one can show very easily that the nucleon operators satisfy the following anticommutation relations

$$\{\hat{B}_n, \hat{B}_{n'}^\dagger\} = \delta_{nn'} - \hat{\Delta}_{nn'}, \qquad \{\hat{B}_n, \hat{B}_{n'}\} = 0 \tag{4.6}$$

where

$$\hat{\Delta}_{nn'} = 3\Psi_n^{*\mu_1\mu_2\mu_3} \Psi_{n'}^{\mu_1\mu_2\nu_3} \hat{q}_{\nu_3}^\dagger \hat{q}_{\mu_3} - \frac{3}{2} \Psi_n^{*\mu_1\mu_2\mu_3} \Psi_{n'}^{\mu_1\nu_2\nu_3} \hat{q}_{\nu_3}^\dagger \hat{q}_{\nu_2}^\dagger \hat{q}_{\mu_2} \hat{q}_{\mu_3} \tag{4.7}$$

For point-like nucleons, the operator $\hat{\Delta}_{nn'}$ would be zero and we would obtain the traditional anticommutation relations for the nucleon creation and annihilation operators. The operator operator $\hat{\Delta}_{nn'}$ is nonzero when the two nucleons can overlap. It is a *quark exchange symmetry* effect due to the Pauli exclusion principle *at the quark level*. One consequence of this noncanonical nature of the anticommutation relation is that the normalization of two nucleon states are not the usual ones, namely:

$$N_{nn'} = \langle nn'|nn'\rangle = 1 - \delta_{nn'} - \Delta N_{nn'} \tag{4.8}$$

where

$$\Delta N_{nn'} = 3\Psi_n^{*\mu_1\mu_2\mu_3} \, \Psi_{n'}^{*\nu_1\nu_2\nu_3} \, \left(\Psi_n^{\mu_1\mu_2\nu_3} \, \Psi_{n'}^{\nu_1\nu_2\mu_3} - \Psi_n^{\mu_1\nu_2\nu_3} \, \Psi_{n'}^{\nu_1\mu_2\mu_3}\right) \tag{4.9}$$

The first two terms in Eq. (4.8) are the usual ones one would obtain if the nucleon operators satisfy canonical anticommutation relations, the other term, $\Delta N_{nn'}$, that involves the three-quark wave functions, is due to the superposition of the quark structure of the two nucleons. The importance of such a superposition increases with the size of the wave functions. The first term in $N_{nn'}$ refers to single-quark exchange and the second to two-quark exchange between the two nucleons.

Now we get to our point; the expectation value of the kinetic energy operator $\hat{K}$ in the two-nucleon state $|nn'\rangle$ receives two types of contributions:

$$\frac{\langle nn'|\hat{K}|nn'\rangle}{N_{nn'}} = \frac{1}{N_{nn'}}\left(K_n + K_{n'} + \Delta K^{Pauli}_{nn'}\right) \tag{4.10}$$

where the two first terms are the single-nucleon contribution given by the expectation value

$$K_i = \langle i|\hat{K}|i\rangle, \qquad i = n, n' \tag{4.11}$$

and $\Delta^{\mathrm{Q\,ex}}_{nn'}$ is the two-nucleon contribution

$$\begin{aligned}\Delta K^{Pauli}_{nn'} = & -3\left[K(\mu_1) + K(\mu_2) + K(\mu_3)\right] \Psi^{*\mu_1\mu_2\mu_3}_{n}\,\Psi^{*\nu_1\nu_2\nu_3}_{n'} \\ & \times \left(\Psi^{\mu_1\mu_2\nu_3}_{n}\,\Psi^{\nu_1\nu_2\mu_3}_{n'} - \Psi^{\mu_1\nu_2\nu_3}_{n}\,\Psi^{\nu_1\mu_2\mu_3}_{n'}\right)\end{aligned} \tag{4.12}$$

Again, $\Delta K^{Pauli}_{nn'}$ is due to the superposition of the nucleon wave functions and obviously depends on the extension of the nucleon wave function. This term gives corrections to EoSs derived on the basis of a single-nucleon approximation, as the ones we have been considering so far. Of course, to be a “correction", the overlap of the two nucleons can not be substantial. A quantitative assessment of the impact of such a correction to the EoS of the Walecka model was carried out in Refs. [23] and [24] using a non-relativisticvistic constituent quark model for the nucleons. Here, we assess the impact of such a correction in the equation of state for the NLWM. As we will see, the effect of such a correction is opposite to the one found for the traditional Walecka model, in the direction of stiffening the EoS.

4.1 Explicit calculation - quark model

Approaches employing a non-relativistic quak-model Hamiltonian have proven effective in describing the properties of hadrons. They explain well the mass spectrum and magnetic properties of individual hadrons [57]. These methods have also been successfully applied to understand multihadron systems, such as in calculating the nucleon-nucleon scattering properties [58].

We outline the calculation in Refs. [23] and [24]. The basic idea is to go from the independent-particle description to an independent-pair description [59], in that one considers the superposition of two nucleons a time only and neglects multinucleon overlaps. The initial step is to compute the energy shift of a given single nucleon n due to its overlap with all the other n' nucleons in nuclear matter (we follow the notation of those references):

$$\Delta E_n^{Pauli} = \sum_{n'} \Delta E_{nn'}^{Pauli} \tag{4.13}$$

where the sum over n' goes up to the Fermi momentum and $\Delta E_{nn'}^{Pauli}$ is given by

$$\Delta E_{nn'}^{Pauli} = \frac{1}{N_{nn'}} \left(\langle nn'|\hat{H}|nn'\rangle - E_n - E_{n'} \right) \tag{4.14}$$

where $\hat{H}$ is the quark model Hamiltonian and E_n is the single-particle energy

$$E_n = \langle n|\hat{H}|n\rangle \tag{4.15}$$

The Hamiltonian is the sum of a kinetic energy $\hat{K}$, Eq. (4.1), and a potential energy. The authors of Refs. [23] and [28] neglect the change in the potential energy with the following argument. The quark-quark interaction depends on the quark density distribution (recall the expression of the potential energy in the second quantization formalism); for two nucleons, we have the overlap of the quark density distributions; from Hartree-Fock theory of many-body physics, one knows that exchange symmetry does not change the density distribution; as such, quark exchange symmetry will not change the potential energy.

Although the potential is not relevant for the energy shift due to the quark exchange symmetry, one does need to specify one to obtain the radial part of the wave functions Ψ_n. The authors of Refs. [23] and [28] use a simple spin-flavor-independent harmonic potential so that the wave functions are given by the product of two Gaussian functions in the relative coordinates and a plane wave in the center-of-mass coordinate. The calculation is relatively straightforward, but it is too long to be repeated here, and so we quote only the final result in the following.

After summing over all internal quantum numbers, color, spin, flavor, and relative momenta, the result for the energy shift can be expressed as (we stress we are using the notation of Ref. [28]):

$$\Delta E_{\tau k}^{Pauli}(k_{F,n}, k_{F,p}) = \sum_{\tau'=n,p} \sum_{\alpha=1,2} c_{\tau\tau'}^{(\alpha)} W_\alpha(k, k_{F,\tau'}) \tag{4.16}$$

where $k_{F,\tau}$ is the Fermi momentum of a nucleon with isospin projection $\tau = n, p$ and, as usual, is given in terms of the medium density n_τ by $k_F = \left(3\pi^2 n_\tau\right)^{1/3}$. The indices $\alpha = 1, 2$ in $c^{(\alpha)}$ and W_α refer to one and two quark exchanges—see the end of the paragraph just above Eq. (4.10). The coefficients $c^{(\alpha)}_{\tau\tau'}$ arise from summing over color, spin and flavor of the quarks and their values are given in the table below [28].

τ	$c^{(1)}_{n\tau}$	$c^{(2)}_{n\tau}$
n	$\frac{15}{81}$	$-\frac{16}{81}$
p	$\frac{12}{81}$	$-\frac{14}{81}$

The functions $W_\alpha(k, k_{F,\tau'})$ result from the integration over the internal quark relative momenta. The analytical derivation of these functions (they can be obtained in closed form in the case of Gaussian wave functions) is detailed in the Appendix of Ref. [28] and the result is:

$$\begin{aligned} W_\alpha(k, k_{F\tau'}) \quad = \quad & \frac{9\sqrt{3}}{64\sqrt{\pi}} \frac{b}{m} \frac{1}{\lambda_\alpha^3} \left\{ 12\sqrt{\pi}[\mathrm{erf}(\lambda_\alpha(k_{F\tau'} - k)) + \mathrm{erf}(\lambda_\alpha(k_{F\tau'} + k))] \right. \\ & + \frac{1}{\lambda_\alpha k} \left\{ [11 - 2\lambda_\alpha^2 k_{F\tau'}(k_{F\tau'} + K)] e^{-\lambda_\alpha^2 (k_{F\tau'} + K)^2} \right. \\ & \left. \left. - [11 - 2\lambda_\alpha^2 k_{F\tau'}(k_{F\tau'} - K)] e^{-\lambda_\alpha^2 (k_{F\tau'} - K)^2} \right\} \right\} \end{aligned} \tag{4.17}$$

Here, m represents the mass of the constituent quark, b is the parameter defining the width of the nucleon's wave function, and $\lambda_\alpha = \alpha \left(b/2\sqrt{3}\right)$.

Ref. [28] takes $b = 0.59$ fm and $m = 350$ MeV, which are typical values of the quark model. We use the same values; there is not much to gain using different values because we are not interested in this dissertation in precise fittings.

To assess typical values of the W_α functions, it is sufficient to consider only the case in which both arguments are equal to the Fermi momentum, that is:

$$W_\alpha(x_{\alpha,F}) = W_\alpha(x_{\alpha,F}, x_{\alpha,F}) = \overline{W}_\alpha K(x_{\alpha,F}) \tag{4.18}$$

with $\overline{W}_\alpha = \frac{9\sqrt{3}}{64\sqrt{\pi}} \frac{b}{m} / \lambda_\alpha^3$, $x_\alpha = \lambda_\alpha k$ is dimensionless momentum and

$$K(x) = 12\sqrt{\pi}\mathrm{erf}(2x) + \frac{1}{x}\left[e^{-4x^2}(11 - 4x^2) - 11\right] \tag{4.19}$$

is the Pauli blocking function that describes how the momentum exchange of quarks between the two nucleons varies with density. A low density expansion of

$K(x)$ is given by

$$K(x) = 40x^3 - \frac{1088}{15}x^5 + \frac{608}{7}x^7 - \frac{3584}{45}x^9 + \frac{4436}{99}x^{11} - \mathcal{O}(x^{13}) \tag{4.20}$$

An accurate fit to the exact result of Eq. (4.19) is provided by the equation:

$$K(x) \approx 12\sqrt{\pi}\left[1 - \left(1 + \frac{10}{3\sqrt{\pi}\gamma}x^3\right)^{-\gamma}\right] \quad , \quad \gamma = 0.35 \tag{4.21}$$

Having a simple form for this function is very convenient because it allows us to avoid evaluate the error function numerically when calculating the energy shift for different densities.

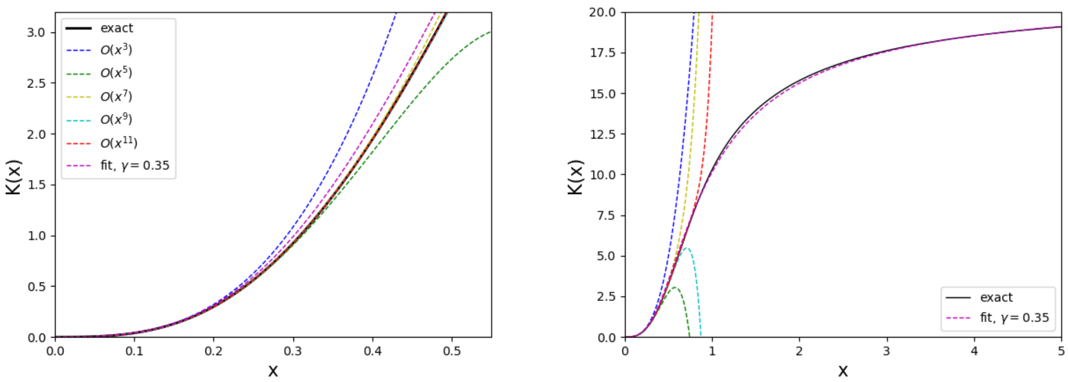

Figure 4.1: The function $K(x)$, described by Eq. (4.19), along with its polynomial expansions described by Eq. (4.20) and the fitting formula given by Eq. (4.21). Left panel: Low densities, Right panel: full range of densities relevant for neutron stars. Results are for $b = 0.59$ fm and $m = 350$ MeV.

The function $K(x)$ is shown in Fig. 4.1; the left panel is for low densities and the right panel is for large densities. In this figure, we compare the exact expression with those using power-law expansion for different expansion powers and the fitting formula. Inspection of the figure reveals that the power-law expansion makes sense only for very low densities. For densities relevant for a neutron star, it fails to capture the fact that the function asymptotically approaches the constant $12\sqrt{\pi}$, approximately 21.269, as one can see on the right panel of Fig. 4.1.

4.2 Results: EoS for the NLWM + quark-exchange

In this section, we present the results of the impact of the energy shift due to quark exchange on the EoS for nuclear matter and pure-neutron matter. The energy shift, Equation (4.16), for symmetric nuclear matter (SNM) ($k_{F,p} = k_{F,n} = k_F$) is given by

$$\Delta E^{Pauli}_{nk_F}(k_F, k_F) = c^{(1)}_{nn}\, W_1(\lambda_1 k_F) + c^{(2)}_{nn}\, W_2(\lambda_2 k_F) + c^{(1)}_{np}\, W_1(\lambda_1 k_F) + c^{(2)}_{np}\, W_2(\lambda_2 k_F) \tag{4.22}$$

and for pure-neutron matter (PNM) ($k_{F,p} = 0$ and $k_{F,n} = k_F$), it is given by

$$\Delta E^{Pauli}_{nk_F}(k_F, k_F) = c^{(1)}_{nn}\, W_1(\lambda_1 k_F) + c^{(2)}_{nn}\, W_2(\lambda_2 k_F) \tag{4.23}$$

Figure 4.2 displays the energy shift for both cases. We stress that the results are for $b = 0.59$ fm and $m = 350$ MeV.

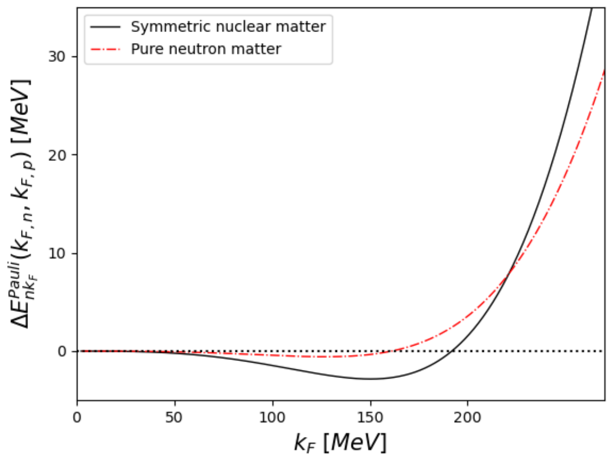

Figure 4.2: Pauli-shifts for symmetric nuclear matter and pure neutrons matter.

One sees the effect due to quark exchange is attractive at low densities and repulsive at high densities. It is attractive at low densities because of the definition in Eq. (4.14). In the actual calculation, the $1/N_{nn'}$ is expanded up to first order in overlap ΔN; therefore one has that the energy shift is $\Delta E^{Pauli} = \Delta K_{nn'} - (E_n + E_{n'})\Delta N_{nn'}$. For low densities, the term $(E_n + E_{n'})\Delta N_{nn'}$ wins over the first one because the first one involves integrations over squared momenta (kinetic energy) and the other involves integration over unity. Now for high density, the situation is the opposite; the integration range becomes larger, and the first integral wins.

This is similar to the short-distance repulsion seen in atoms: at short inter-atom distances (high relative momenta), the two-atom energy increases substantially; the physical reason is that the Pauli principle at the electron level demanding anti-symmetrization induces high momentum components in the relative wave function.

The modification of the Walecka model with the effects of quark exchange (Pauli blocking) among nucleons is simply adding extra terms of pressure and energy density to the Eqs. (3.75) and (3.78). Note that an energy shift is a shift in the chemical potential. Therefore:

$$
\begin{aligned}
P &= \frac{1}{2}\frac{g_\omega^2}{m_\omega^2}n_B^2 - \frac{1}{2}\frac{g_\sigma^2}{m_\sigma^2}n_s^2 \\
&+ \frac{1}{4\pi}\left[\left(\frac{2}{3}k_F^3 - (m_N^*)^2 k_F\right)E_F^* + (m_N^*)^2 \ln\left(\frac{k_F + E_F^*}{m_N^*}\right)\right] + P_{ex} \qquad (4.24)
\end{aligned}
$$

$$
\begin{aligned}
\epsilon &= \frac{1}{2}\frac{g_\omega^2}{m_\omega^2}n_B^2 + \frac{1}{2}\frac{g_\sigma^2}{m_\sigma^2}n_s^2 \\
&+ \frac{1}{4\pi^2}\left[(2k_F^3 + (m_N^*)^2 k_F)E_F^* - (m_N^*)^4 \ln\left(\frac{k_F + E_F^*}{m_N^*}\right)\right] + \epsilon_{ex} \qquad (4.25)
\end{aligned}
$$

where

$$
\begin{aligned}
\mu_\tau &= E_\tau^* + \frac{g_\omega^2}{m_\omega^2}n_\tau + \mu_{ex,\tau} && (4.26)\\
\mu_{ex,\tau} &= \Delta_\tau(n,x) = \Delta E^{Pauli}_{\tau k_{F,\tau}}(k_{F,n}, k_{F,p}) && (4.27)\\
\epsilon_{ex} &= \int_0^n dn' \{x\Delta_p(n',x) + (1-x)\Delta_n(n',x)\} && (4.28)\\
P_{ex} &= \sum_{\tau=n,p} \mu_{ex} n_\tau - \epsilon_{ex} && (4.29)
\end{aligned}
$$

where $n_p(n_n)$ denotes the proton(neutron) baryon density and $x = n_p/n_B$ ($n_B = n_p + n_n$) is the proton fraction.

Equations (3.73) and (3.80) defining the effective nucleon mass m_N^* and the scalar density n_s still hold. We then readjust the parameters g_σ and g_ω to obtain the correct saturation properties of nuclear matter. In the case of the NLWM, we do not change the couplings b and c of the scalar self-interactions, Eq. (3.94). The first and most important reason is the lack of sufficient astrophysical data to constrain such terms. Second, while these terms are governed by the scalar density, the quark exchange symmetry contribution is governed by the vector density (baryon density); as such, we expect that only the mean-field couplings will be affected, and among those, the g_ω should be more modified. In fact, while keeping the b and c couplings fixed, the new couplings are $g_\sigma^2/4\pi = 2.931$ and $g_\omega^2/4\pi = 1.544$, confirming that the value of the coupling g_ω changes more than that of g_σ.

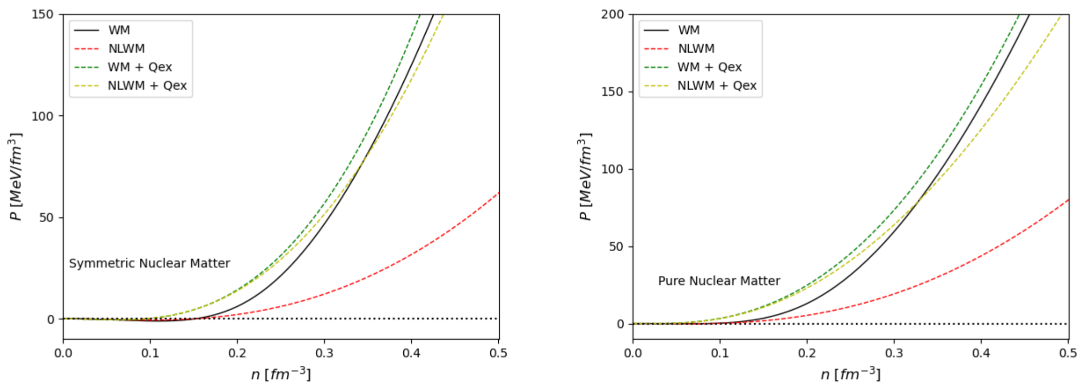

Figure 4.3: Pressure as a function of baryon density. Left panel: Symmetric nuclear matter. Right panel: Pure-neutron matter.

Figure 4.3 displays the pressure as a function of the baryon density for nuclear matter (left panel) and neutron matter (right panel) predicted by the models we considered, without and with quark exchange (Qex): WM, WM + Qex, NLWM and NLWM + Qex. One clearly sees an opposite effect that quark exchange has on the pressure: while in the Walecka model it decreases the pressure (softens), in the NLWM it increases the pressure (stiffens). This is a welcome feature in view of the fact that a stiffer equation of state, rising rapidly with a density around 2.4 times the normal nuclear matter saturation density, is required [29] to accommodate the recent NICER measurement of the radius of the neutron star PSR J0740 + 6620 [30]. That density is in the regime where it is expected that hadronic matter transforms into quark matter. As mentioned earlier, quark exchange is a precursor phenomenon to the transition to fully deconfined quark matter. The required pressure in that density regime is greater than predicted by state-of-the-art microscopic nuclear many-body calculations of nuclear matter. An stiff equation of state is needed.

In Fig. 4.4 we present the results for the binding energy per nucleon as a function of baryon density for the same models. The message is the same, Qex has an opposite effect in the models. Recall that the Walecka model yielded a value for the incompressibility of approximately 550 MeV, including quark exchange,

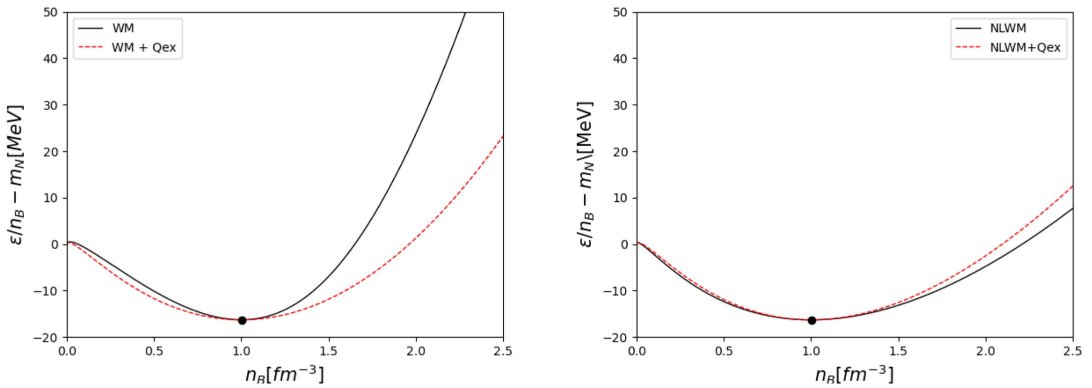

Figure 4.4: Binding energy per particle as a function of the n_B. Left panel: Walecka model. Right panel: Walecka Model including scalar interactions (NLWM).

it goes down to 330 MeV. The situation is reversed in the case of the NLWM, the incompressibility increases from 250 MeV to 295 MeV, indicating a stiffening of the EoS.

At this point, it is worth mentioning that the use of two separate models to incorporate quark exchange at high densities might be avoided by the use of a model formulated *ab initio* in terms of quark degrees of freedom. One of such models is the quark-meson-coupling (QMC) model. This is a model for nuclear matter and finite nuclei built on quark degrees of freedom confined in nucleons interacting with scalar and vector mean fiels; it was originally proposed in Ref. [60] and subsequently applied in the description of a variety of nuclear phenomena [61]. The incorporation of quark exchange is very natural within such a model and does not require any additional ingredients [25].

4.3 Results: the Mass-Radius Relation

Again solving the TOV equation, Eq. (3.10), for the equation of state expressed by the Eqs. (4.25) and (4.24), without enforcing β-equilibrium, we obtain the following results:

$M_{max}[M_0]$	2.592
$R_{max}(\text{Km})$	12.942

We see that including quark exchange, the maximum allowable mass is approximately $2.6M_\odot$, which so far can indeed describe a real neutron star. The mass-radius relation is presented in Fig. 4.5, left panel.

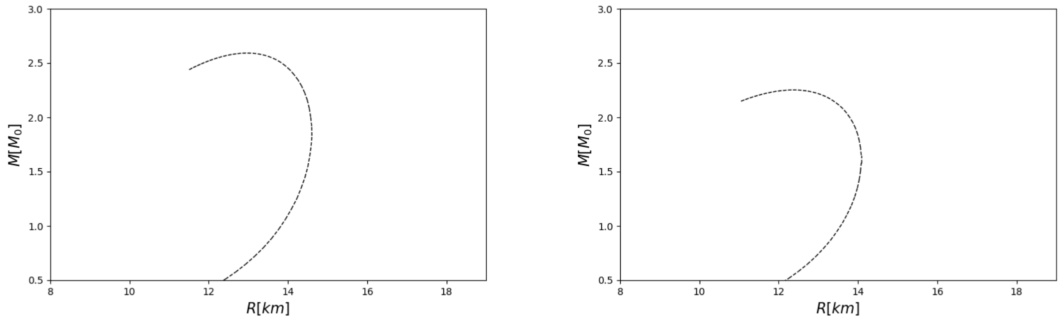

Figure 4.5: Mass-radius relation. Left panel: WM+Qex. Right panel: NLWM+Qex

On the other hand, what we obtain in the model when we add scalar self-interactions interactions, the results are given in the table below:

$M_{max}[M_0]$	2.252
R_{max}(Km)	12.324

This values for the mass of $2.225 M_\odot$ and radius should compared to the corresponding accepted values for the neutron star PSR J0952-0607: $M = 2.35 \pm 0.17\ M_\odot$ and $R = 14.087 \pm 1.0186$ Km. The mass-radius relationship is plotted in Fig. 4.5, right panel. Given the simplicity of the calculations, one can assume that the results are well within the range of the current observations.

Chapter 5

Conclusion

Our primary aim in this dissertation was to present a review on the properties of neutron stars and used two relativistic quantum field theories to obtain the equation of state of dense matter. We also make an original contribution to the field by evaluating the contribution of quark exchange to the equation of state of dense baryonic matter. Initially, we developed several equations of state to solve the well-known structural equations that describe a spherically symmetric star in hydrostatic equilibrium, derived from the theory of general relativity - the so-called Tolman-Oppenheimer-Volkov (TOV) equation.

Starting from the original Walecka model (WM), which involves the interaction between hadrons through Yukawa couplings to scalar and vector mesons, we obtained the equation of state (EoS) of nuclear matter and pure-neutron matter, and then computed the mass-radius relation of neutrons stars. This first exercise allowed us to review the basic tools of finite temperature field theory to compute the EoS. The fact that this model predicts an incompressibility of nuclear matter that is too high compared to those extracted experimentally for large nuclei, we increased the complexity of the model by introducing higher-order interactions between scalar mesons, specifically cubic and quartic interactions. They represent physically three- and four-nucleon forces, which are important ingredients to describe high density matter. Adding those terms leads to the nonlinear Walecka model (NLWM), as the model is known in the literature.

Next, we extended these models to incorporate contributions from quark exchange and examined their influence on the equation of state. Quark exchange in the nuclear medium is a precursor phenomenon to fully deconfined quark matter. The central result of our calculation is that one obtains a stiffer equation of state than the one predicted by the NLWM, which, we recall, is a richer model than the traditional WM as it contains many-body forces that play an important role at high nuclear densities. Our finding hints that quark exchange might be relevant in this respect in view of the fact that a stiffer EoS, with stiffness increasing rapidly with a density around 2.4 times the normal saturation density, seems to be required to understand recent astrophysical data. A density 2.4 times the normal saturation density is within the range of densities than one expects that hadronic matter transforms into quark matter.

Finally, the findings in this analysis underscore the importance and variety of strategies employed in effective field theories. Thus, despite oversimplifications, the results of this study not only reinforce established knowledge but also bring insight and provide valuable guidance for subsequent more elaborate research, fostering the enhancement of our understanding of neutron stars.

As for future work, in order to make our description of neutron stars more realistic, we can enhance and refine the results found so far by:

- Adding to the Lagrangian an isovector-vector meson, the ρ meson, which allows us to take into account the large isospin asymmetry and obtain a more realistic symmetry energy.
- Taking into account β-equilibrium as is essential for real stars.
- Adding the effect of the magnetic field on the structural equations of general relativity, as it is necessary for strong fields and, as the field possesses energy itself it disrupts the spherical symmetry of the star.
- Adding the effects of rotation is essential, as neutron stars have a large angular momentum, which also disrupts their spherical symmetry.
- Using a model built on explicit quark degrees of freedom avoids dealing with two separate models and opens new perspectives in this field.

Appendix A

Thermal Field Theory for Boson and Fermion fields

Thermal Field Theory is an extension of conventional quantum field theory, which takes into account the influence of temperature on the quantum states of the system. This formalism is essential for understanding phenomena in physical systems that are in thermal equilibrium, allowing the description of quantum systems under finite-temperature conditions.

This appendix aims to provide a concise overview of the fundamental concepts associated with equilibrium thermal field theory, focusing on spin-0 bosonic and spin-1/2 fermionic fields. Although we will not need the partition function with quantum bosonic fields in this dissertation, because we use a mean-field approximation for them in the conxtext of the Walecka model [16], we discuss them here for completeness and contrast with the formalism for fermion fields that we do need in this dissertation, namely Dirac fields representing neutrons and protons. Moreover, the bosons we consider in this dissertation are uncharged scalar and vector bosons, i.e. particles described by real fields. However, again for contrasting with the formalism for fermion fields, we discuss the thermal field theory for a charged scalar field, for which one can associate a chemical potential like in the case of complex fermion fields. The presentation here closely follows the material in the Appendix A of Ref. [54].

The basic quantity of interest is the partition function Z, which is generically given in terms of the Hamiltonian operator $\hat{H}$ and a conserved charge operator $\hat{N}$ by:

$$Z = \mathrm{Tr}\, e^{-\beta(\hat{H}-\mu\hat{N})} \tag{A.1}$$

where $\beta = 1/T$ (recall that we are using units such that Boltzmann's constant is equal to unity) and μ is the chemical potential associated with conserved charge $\hat{N}$. In the following, we show how the trace can be expressed in terms of a functional integral over the field variables.

In the mean-field approximation of the Walecka model, one needs the partition function only for a quadratic fermionic action. For this reason, in this appendix we consider only quadratic actions.

A.1 Boson Field

We start from the Lagrangian density for a complex scalar field φ in Minkowski space :

$$\mathcal{L} = \partial_\mu \varphi^* \partial^\mu \varphi - m^2 \varphi^* \varphi \tag{A.2}$$

To construct the Hamiltonian, we need the conjugate momentum Π to the field φ, which is given by:

$$\Pi = \frac{\partial \mathcal{L}}{\partial(\partial_0 \varphi)} = \partial_0 \varphi \tag{A.3}$$

from which, we get for the Hamiltonian density $\mathcal{H}$:

$$\mathcal{H} = \Pi \varphi^* + \Pi^* \varphi - \mathcal{L} = \Pi^* \Pi + \nabla \varphi^* \cdot \nabla \varphi + U(\varphi^* \varphi)$$

Next, we need the conserved charge. We see that $\mathcal{L}$ is invariant under $U(1)$ rotations of the field:

$$\varphi \to e^{i\alpha} \varphi \tag{A.4}$$

This invariance yields a conserved the Noether current

$$J^\mu = i \left(\varphi^* \partial^\mu \varphi - \varphi \partial^\mu \varphi^* \right) \tag{A.5}$$

with the corresponding conserved charge N given by:

$$N = \int d^3x \, \mathcal{N}(x) \tag{A.6}$$

where $\mathcal{N}$ is the charge density

$$\mathcal{N} = J^0 = i \left(\varphi^* \partial^0 \varphi - \varphi \partial^0 \varphi^* \right) \tag{A.7}$$

It is convenient to express the complex fields φ and φ^* in terms of two real fields, φ_1 and φ_2, as follows:

$$\varphi = \frac{1}{\sqrt{2}} (\varphi_1 + i \varphi_2) \tag{A.8}$$

Then, the Lagrangian becomes

$$\mathcal{L} = \frac{1}{2}\left[\partial_\mu\varphi_1\partial^\mu\varphi_1 + \partial_\mu\varphi_2\partial^\mu\varphi_2 - m^2(\varphi_1^2 + \varphi_2^2)\right] \tag{A.9}$$

The conjugate momenta fields Π_1 and Π_2 corresponding to the fields φ_1 and φ_2 are given by

$$\Pi_i = \frac{\partial\mathcal{L}_0}{\partial(\partial_0\varphi_i)} = \partial^0\varphi_i, \qquad i = 1,2 \tag{A.10}$$

Therefore, one obtains for the Hamiltonian density $\mathcal{H}$:

$$\begin{aligned}\mathcal{H} &= \Pi_1\partial_0\varphi_1 + \Pi_2\partial_0\varphi_2 - \mathcal{L}\\ &= \frac{1}{2}\left[\Pi_1^2 + \Pi_2^2 + (\nabla\varphi_1)^2 + (\nabla\varphi_2)^2 + m^2(\varphi_1^2 + \varphi_2^2)\right]\end{aligned} \tag{A.11}$$

and for the charge density $\mathcal{N}$:

$$\mathcal{N} = \varphi_2\Pi_1 - \varphi_1\Pi_2 \tag{A.12}$$

Therefore, one can now compute the trace in the bases of the eigenstates of the fields φ_1 and φ_2 following the same steps for a real scalar field [62, 55].

The result o such a computation is given by [62]:

$$\begin{aligned}Z &= \mathrm{Tr}\, e^{-\beta(\hat{H}-\mu\hat{N})}\\ &= \int \mathcal{D}\Pi_1\mathcal{D}\Pi_2 \int_{\text{periodic}} \mathcal{D}\varphi_1\mathcal{D}\varphi_2 \exp\left\{\int_X \left[i\Pi_1\partial_\tau\varphi_1 + i\Pi_2\partial_\tau\varphi_2\right.\right.\\ &\quad - \frac{1}{2}\left(\Pi_1^2 + \Pi_2^2 + (\nabla\varphi_1)^2 + (\nabla\varphi_2)^2 + m^2(\varphi_1^2 + \varphi_2^2)\right)\\ &\quad \left.\left. + \mu\left(\varphi_2\Pi_1 - \varphi_1\Pi_1\right)\right]\right\}\end{aligned} \tag{A.13}$$

where we have abbreviated the integration symbol over spatial $\mathbf{x}$ and "imaginary time" τ variables as

$$\int_X (\cdots) \equiv \int_0^\beta d\tau \int d^3x\, (\cdots) \tag{A.14}$$

Also, as indicated in (A.13), the functional integral has to be performed over fields that are periodic in the τ variable, with the period given by β:

$$\varphi_1(0,\mathbf{x}) = \varphi_1(\beta,\mathbf{x}) \quad \text{and} \quad \varphi_2(0,\mathbf{x}) = \varphi_2(\beta,\mathbf{x}) \tag{A.15}$$

A simple way to see how this periodicity arises is to recall that the quantum mechanical trace computed in the basis of the field operator, which leads to the functional integral, can be thought of as a quantum mechanical transition amplitude computed with initial and final states at the same "time" [55].

Next, one integrates out the conjugate momenta, and, up to an overall constant, one obtains for the partition function:

$$\begin{aligned} Z = \int_{\text{periodic}} \mathcal{D}\varphi_1 \mathcal{D}\varphi_2 \exp\Bigg\{ \int_X \Bigg[-\frac{1}{2}\Big((\partial_\tau \varphi_1)^2 + (\nabla\varphi_1)^2 + (\partial_\tau\varphi_2)^2 + (\nabla\varphi_2)^2 \Big) \\ -\frac{1}{2}(m^2-\mu^2)\left(\varphi_1^2+\varphi_1^2\right) + i\mu(\partial_\tau\varphi_1\,\varphi_2 - \partial_\tau\varphi_2\,\varphi_1) \Bigg]\Bigg\} \end{aligned} \tag{A.16}$$

To compute the functional integrals, it is convenient to introduce the Fourier transforms of the fields:

$$\varphi_i(X) = \frac{1}{\sqrt{TV}} \sum_K e^{-iK\cdot X} \varphi_i(K) = \frac{1}{\sqrt{TV}} \sum_K e^{i(\omega_n \tau + \mathbf{k}\cdot\mathbf{x})} \varphi_i(K), \qquad i = 1,2 \tag{A.17}$$

where we follow Ref. [54] which uses four-momentum notation with the understanding that

$$K \equiv (-i\omega_n, \mathbf{k}) \quad \text{and} \quad K\cdot X \equiv k^0 x^0 - \mathbf{k}\cdot\mathbf{x} = -(\omega_n\tau + \mathbf{k}\cdot\mathbf{x}) \tag{A.18}$$

$$K^2 = K\cdot K = -\left(\omega_n^2 + \mathbf{k}^2\right) \tag{A.19}$$

The normalization is chosen such that the Fourier-transformed fields $\varphi_i(K)$ are dimensionless. Since the fields φ_i are real, we that their Fourier transforms have the property $\varphi_i(-K) = \varphi^*(K)$, which will be used shortly ahead.

The 0^{th} component of the four-momentum is given by the Matsubara frequencies ω_n; which due to the periodicity requirement $\varphi(0,\mathbf{x}) = \varphi(\beta,\mathbf{x})$, they satisfy $e^{i\omega_n\beta} = 1$, that is, the $\omega_n\beta$ must be integers multiple of 2π, or

$$\omega_n = 2\pi n T, \qquad n \in \mathbb{Z} \tag{A.20}$$

Next, we replace the Fourier transformed fields in (A.16). We perform these integrals. We start with those involving the derivatives and the combination

$\overline{m}^2 \equiv m^2 - \mu^2$, namely:

$$I_1 = \int_X \left[(\partial_\tau \varphi_i)^2 + (\nabla \varphi_i)^2 + \overline{m}^2 \varphi_i^2 \right] = \sum_{n,n'} \sum_{\mathbf{k},\mathbf{k}'} \varphi_i(K')\varphi_i(K)$$
$$\times \left(-\omega_n \omega_{n'} - \mathbf{k} \cdot \mathbf{k}' + \overline{m}^2 \right) \frac{1}{T} \underbrace{\int_0^\beta d\tau \, e^{i(\omega_n + \omega_{n'})\tau}}_{A} \frac{1}{V} \underbrace{\int_V d^3x \, e^{i(\mathbf{k}+\mathbf{k}') \cdot \mathbf{x}}}_{B} \tag{A.21}$$

The A and B integrals are easily computed:

$$\begin{aligned} A &= \int_0^\beta d\tau e^{i(\omega_n + \omega_{n'})\tau} = \int_0^\beta d\tau e^{2\pi i (n+n')T\tau} \\ &= \frac{1}{2\pi i (n+n')T} \left[e^{2\pi i (n+n')T\tau} \right]_0^\beta = \frac{1}{2\pi i (n+n')T} \left[e^{2\pi i (n+n')} - 1 \right] \\ &= \frac{1}{T} \delta_{n',-n} \end{aligned} \tag{A.22}$$

$$B = \int_V d^3x \, e^{i(\mathbf{k}+\mathbf{k}') \cdot \mathbf{x}} = V \, \delta_{\mathbf{k}',-\mathbf{k}} \tag{A.23}$$

Using these results in (A.21), one then obtains:

$$I_1 = \sum_{n,\mathbf{k}} \varphi_i(-K) \, \frac{\omega_n^2 + \mathbf{k}^2 + \overline{m}^2}{T^2} \, \varphi_i(K) \tag{A.24}$$

The integrals proportional to μ can be done in the same manner, with the result:

$$\begin{aligned} I_2 &= \int_{\mathbf{x}} \left(\partial_\tau \varphi_1 \, \varphi_2 - \partial_\tau \varphi_2 \, \varphi_1 \right) = \sum_{n,n'} \sum_{\mathbf{k},\mathbf{k}'} \left(\varphi_1(K')\varphi_2(K) - \varphi_2(K')\varphi_1(K) \right) \, i\omega_{n'} \\ &\times \frac{1}{T} \int_0^\beta d\tau \, e^{i(\omega_n + \omega_{n'})\tau} \, \frac{1}{V} \int_V d^3x \, e^{i(\mathbf{k}+\mathbf{k}') \cdot \mathbf{x}} \\ &= \sum_{n,\mathbf{k}} \left[\varphi_1(-K) \, \frac{-i\omega_n}{T^2} \, \varphi_2(K) - \varphi_2(-K) \, \frac{-i\omega_n}{T^2} \, \varphi_1(K) \right] \\ &= -\frac{1}{2} \sum_{n,\mathbf{k}} \begin{pmatrix} \varphi_1(-K) & \varphi_2(-K) \end{pmatrix} \begin{pmatrix} 0 & \frac{2i\omega_n}{T^2} \\ -\frac{2i\omega_n}{T^2} & 0 \end{pmatrix} \begin{pmatrix} \varphi_1(K) \\ \varphi_2(K) \end{pmatrix} \end{aligned} \tag{A.25}$$

With these results for the integrals I_1 and I_2, one can write the partition function as

$$Z = \int \mathcal{D}\varphi_1 \mathcal{D}\varphi_2 \exp \left[-\frac{1}{2} \sum_{n,\mathbf{k}} \begin{pmatrix} \varphi_1(-K) & \varphi_2(-K) \end{pmatrix} \frac{D^{-1}(K)}{T^4} \begin{pmatrix} \varphi_1(K) \\ \varphi_2(K) \end{pmatrix} \right] \tag{A.26}$$

with $D^{-1}(K)$ being the 2×2 matrix:

$$D^{-1}(K) = D^{-1}(n, \mathbf{k}) = \begin{pmatrix} \omega_n^2 + \mathbf{k}^2 + m^2 - \mu^2 & -2\mu\omega_n \\ 2\mu\omega_n & \omega_n^2 + \mathbf{k}^2 + m^2 - \mu^2 \end{pmatrix} \tag{A.27}$$

The easiest way to compute this functional integral is to change variables through a unitary transformation on the fields that diagonalizes the 2×2 matrix $D^{-1}(K)$. Being a unitary transformation, the Jacobian of the transformation is unity. Denoting $d_1(K)$ and $d_2(K)$ the eigenvalues of $D^{-1}(K)$, the functional integral is computed very easily: it is a product of ordinary Gaussian integrals $I_G([d_i(K)]$ of the form

$$I_G[d_i(K)] = \int_{-\infty}^{\infty} dx\, e^{-\frac{1}{2}\left(d_i(K)/T^2\right) x^2} = (2\pi)^{1/2} \left(d_i(K)/T^2\right)^{-1/2}, \quad i = 1, 2 \tag{A.28}$$

It is not difficult to show that the result for the partition function, up to factors of 2π, can be written in the form:

$$\begin{aligned} Z &= \prod_{n,\mathbf{k}} \left[\left(d_1(K)/T^2\right) \left(d_2(K)/T^2\right) \right]^{-1/2} \\ &= \prod_{n,\mathbf{k}} \left[\left((\epsilon_k^+)^2 + \omega_n^2\right)/T^2 \times \left((\epsilon_k^-)^2 + \omega_n^2\right)/T^2 \right]^{-1/2} \end{aligned} \tag{A.29}$$

where

$$\epsilon_k^{\pm} = E_k \mp \mu \qquad \text{with} \qquad E_k = \left(\mathbf{k}^2 + m^2\right)^{1/2} \tag{A.30}$$

In general, one is interested in the grand canonical potential $\Omega = -T \ln Z/\beta$. Given the above result for Z, we obtain for Ω the following expression:

$$\begin{aligned} \Omega &= -T \ln \prod_{n,\mathbf{k}} \left[\left((\epsilon_k^+)^2 + \omega_n^2\right)/T^2 \times \left((\epsilon_k^-)^2 + \omega_n^2\right)/T^2 \right]^{-1/2} \\ &= -T \sum_{n,\mathbf{k}} \ln \left[\left((\epsilon_k^+)^2 + \omega_n^2\right)/T^2 \times \left((\epsilon_k^-)^2 + \omega_n^2\right)/T^2 \right]^{-1/2} \\ &= \frac{T}{2} \sum_{n,\mathbf{k}} \ln \left[\left((\epsilon_k^+)^2 + \omega_n^2\right)/T^2 \times \left((\epsilon_k^-)^2 + \omega_n^2\right)/T^2 \right] \\ &= \frac{T}{2} \sum_{n,\mathbf{k}} \left[\ln \frac{(\epsilon_k^+)^2 + \omega_n^2}{T^2} + \ln \frac{(\epsilon_k^-)^2 + \omega_n^2}{T^2} \right] \end{aligned} \tag{A.31}$$

We need to perform the sum over the Matsubara frequencies; this will be done in the following subsection.

A.1.1 Sum over Bosonic Matsubara Frequencies

First, let us consider the following resul:

$$I = \sum_n \ln \frac{\omega_n^2 + \epsilon_k^2}{T^2} = \int_1^{(\epsilon_k/T)^2} dx^2 \sum_n \frac{1}{(2n\pi)^2 + x^2} + \sum_n \ln \left[1 + (2n\pi)^2\right] \tag{A.32}$$

Proof:

$$\begin{aligned} I &= \int_1^{(\epsilon_k/T)^2} dy \, \sum_n \frac{1}{(2n\pi)^2 + y} = \sum_n \ln \left[(2n\pi)^2 + y\right]_1^{(\epsilon_k/T)^2} \\ &= \sum_k \ln \frac{\omega_n^2 + \epsilon_k^2}{T^2} - \sum_n \ln \left[1 + (2n\pi)^2\right] \end{aligned} \tag{A.33}$$

Now, we write as a contour integral

$$T \sum_n \frac{1}{\omega_n^2 + \epsilon_k^2} = -\frac{1}{2\pi i} \oint_c d\omega \frac{1}{\omega^2 - \epsilon_k^2} \frac{1}{2} \coth \frac{\omega}{2T} \tag{A.34}$$

The second identify follows from the residue theorem:

$$\frac{1}{2\pi i} \oint_c dz f(z) = \sum_n \mathrm{Res} f(z) \Big|_{z=z_n} \tag{A.35}$$

where the z_n are the poles of $f(z)$ in the area enclosed by the contour C.
Proof: If we can write the function $f(z)$ as $f(z) = \varphi(z)/\psi(z)$, with analytic $\varphi(z)$, $\psi(z)$, the residues are

$$\mathrm{Res} f(z)|_{z=z_n} = \frac{\varphi(z_n)}{\psi'(z_n)} \tag{A.36}$$

with

$$f(\omega) = \frac{1}{2} \frac{1}{\omega^2 - \epsilon_k^2} \coth \frac{\omega}{2T} \tag{A.37}$$

Since

$$\coth x = \frac{e^x + e^{-x}}{e^x - e^{-x}} \tag{A.38}$$

we then can write

$$\varphi(\omega) = \frac{1}{2}\frac{e^{\omega/2T} + e^{-\omega/2T}}{\omega^2 - \epsilon_k^2}, \qquad \psi(\omega) = e^{\omega/2T} - e^{-\omega/2T} \tag{A.39}$$

The contour C is chosen such that it encloses all poles of $\coth \omega/2T$ and none of $1/\omega - \epsilon_k^2$. The poles are given by $e^{\omega/2T} - e^{-\omega/2T} = 0$, that is, they are on the imaginary axis, $\omega = i\omega_n$

$$\mathrm{Res} f(\omega)|_{\omega=i\omega_n} = \frac{\varphi(i\omega_n)}{\psi'(i\omega_n)} = -T\frac{1}{\omega_n^2 + \epsilon_k^2} \tag{A.40}$$

From this results, Eq. (A.34) follows immediately.

Next, we way deform the contour C (which consist of infenitely many circles surrouding the poles) and obtain

$$\begin{aligned} T\sum_n \frac{1}{\omega_n^2 + \epsilon_k^2} &= -\frac{1}{2\pi i}\int_{-i\infty+\eta}^{i\infty+\eta} d\omega \frac{1}{\omega^2 - \epsilon_k^2}\frac{1}{2}\coth\frac{\omega}{2T} \\ &\quad -\frac{1}{2\pi i}\int_{i\infty-\eta}^{-i\infty-\eta} d\omega \frac{1}{\omega^2 - \epsilon_k^2}\frac{1}{2}\coth\frac{\omega}{2T} \\ &= -\frac{1}{2\pi i}\int_{-i\infty+\eta}^{i\infty+\eta} d\omega \frac{1}{\omega^2 - \epsilon_k^2}\coth\frac{\omega}{2T} \end{aligned} \tag{A.41}$$

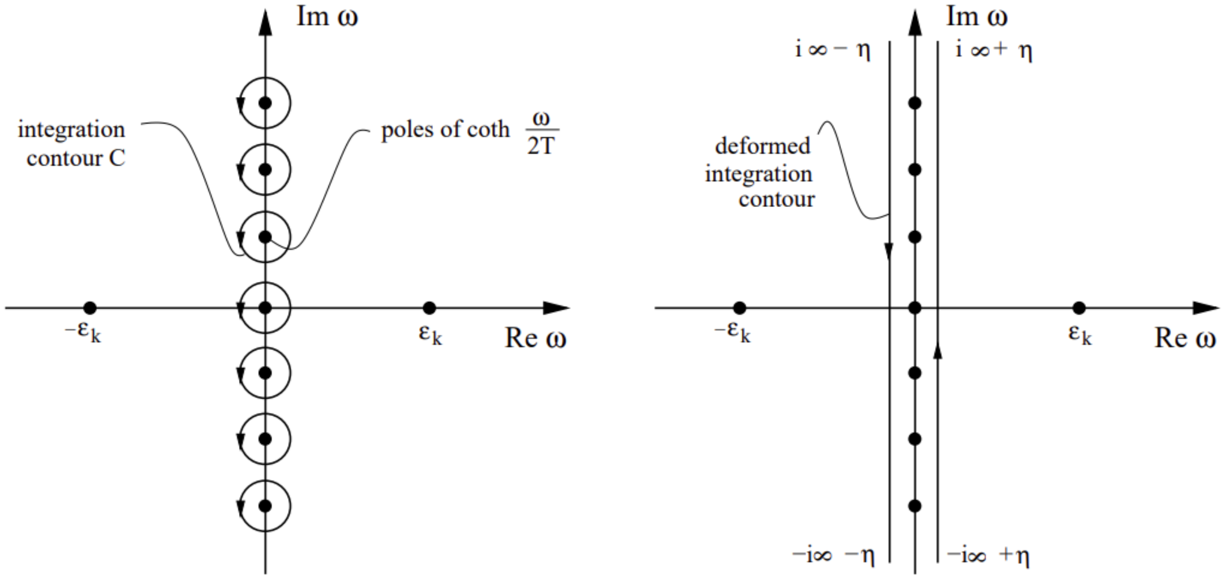

Figure A.1: Left: integration path in the complex ω-plane utilized in Eq. (A.34). Right: modified integration path according to Eq. (A.41) [63].

We now use the residue theorem a second time: We can close the contour in the positive half-plane at infinity and pick up the pole at $\omega = \epsilon_k$,

$$\varphi(\omega) = \coth \frac{\omega}{2T}, \quad \psi(\omega) = \omega^2 - \epsilon^2, \quad \psi'(\omega) = 2\omega \tag{A.42}$$

so that

$$\begin{aligned} T\sum_n \frac{1}{\omega_n^2 + \epsilon_k^2} &= \frac{1}{2\epsilon_k} \coth \frac{\epsilon_k}{2T} = \frac{1}{2\epsilon_k} \left(\frac{e^{\epsilon_k/2T} + e^{-\epsilon_k/2T}}{e^{\epsilon_k/2T} - e^{-\epsilon_k/2T}} \right) \\ &= \frac{1}{2\epsilon_k} \left[\frac{e^{-\epsilon_k/2T}}{e^{-\epsilon_k/2T}} \left(\frac{e^{\epsilon_k/T} + 1}{e^{\epsilon_k/T} - 1} \right) \right] = \frac{1}{2\epsilon_k} \left[1 + \frac{2}{e^{\epsilon_k/T} - 1} \right] \\ &= \frac{1}{2\epsilon_k} [1 + 2f_B(\epsilon_k)], \end{aligned} \tag{A.43}$$

where

$$f_B(\epsilon) \equiv \frac{1}{e^{\epsilon/T} - 1} \tag{A.44}$$

is the *Bose distribution function*. With $\epsilon_k = Tx$, we have

$$T\sum_n \frac{1}{\omega_n^2 + \epsilon_k^2} = \frac{1}{Tx} \left[\frac{1}{2} + \frac{1}{e^x - 1} \right] \tag{A.45}$$

and

$$\sum_n \ln \frac{\omega_n^2 + \epsilon_k^2}{T^2} = c \int_1^{(\epsilon_k/T)^2} dx^2 \, \frac{1}{x} \left(\frac{1}{2} + \frac{1}{e^x - 1} \right) + C \tag{A.46}$$

where C is a constant. Making the change o variables:

$$x^2 = y; \quad u = \sqrt{y}; \quad dy = 2udu \tag{A.47}$$

we can write the integral above as

$$\begin{aligned} 2\int du \left(\frac{1}{2} + \frac{1}{e^u - 1} \right) &= \int du \left(\frac{2e^u}{e^u - 1} - 1 \right) = 2\int dw \frac{1}{w} - \int du \\ &= 2\ln(e^u - 1) - u = 2\ln\left(\frac{1 - e^{-u}}{e^{-u}} \right) - u \\ &= 2\ln(1 - e^{-u}) + u \end{aligned} \tag{A.48}$$

Inserting the limits, one then finally have:

$$\sum_n \ln \frac{\omega_n^2 + \epsilon_k^2}{T^2} = \frac{\epsilon_k}{T} + 2\ln\left(1 - e^{-\epsilon_k/T}\right) + C \tag{A.49}$$

Therefore, neglecting the constant, and taking the thermodynamic limit using the result

$$\sum_{\mathbf{k}} (\cdots) \to V \int \frac{d^3k}{(2\pi)^3} (\cdots) \tag{A.50}$$

we obtain for the grand canonical potential Ω the result:

$$\frac{\Omega}{V} = T \int \frac{d^3\mathbf{k}}{(2\pi)^3} \left[\frac{\epsilon_k^+ + \epsilon_k^-}{2T} + \ln(1 - e^{-\epsilon_k^+/T}) + \ln(1 - e^{-\epsilon_k^-/T}) \right] \tag{A.51}$$

From this expression we can compute the pressure $P = -\Omega/V$. The first term in the integrand yields an infinite contribution which however is T-independent. We way thus use a "renormalization" such that the vacuum pressure vanishes.

A.2 Grassmann variables

Before delving into the problem of deriving the partition function for a fermionic field, we first review the use of Grassmann variables, which, as we will see, are used to represent the fermionic fields in a functional integral. We start considering real variables and then extend them to include complex conjugation, a step necessary for representing Dirac fields in a functional integral.

Let us consider an r-dimensional vector space with the following basis

$$\eta_1, \ldots, \eta_r \tag{A.52}$$

and define an anticommuting product

$$\eta_i \eta_j = -\eta_j \eta_i \tag{A.53}$$

This defines what is called the Grassmann algebra ($\mathcal{A}$). Note that Eq.(A.53) implies that

$$\eta_i^2 = 0 \tag{A.54}$$

We now require a sign convention to establish the notion of derivatives on this space. For instance, in the case of $j \neq k$,

$$\frac{\partial}{\partial \eta_j}\eta_j\eta_k = \eta_k \quad , \quad \frac{\partial}{\partial \eta_k}\eta_j\eta_k = -\eta_j \tag{A.55}$$

We have defined this derivative to act from the left and note that the second-order derivatives of any product of η's result in null values. This already hints that integration on this space differs somewhat from the usual, as the second-order derivative vanishes, implying there is no inverse operation to this differentiation. However, to define these integrals, we will require them to be translationally invariant and linear:

$$\int d\eta f(\eta) = \int d\eta f(\eta + \zeta) \ \ , \ \ \int d\eta(a\eta + b) = a\int d\eta\eta + b\int d\eta \tag{A.56}$$

with $b \in \mathbb{C}$ and $\zeta \in \mathcal{A}$. Within this context, the integration range always spans the entire space. In other words, we can only refer to "definite" integrals since "indefinite" ones would imply the direct existence of an inverse operation to differentiation, which, as we have seen, does not exist. Since the most general way to define a function of η is through $f(\eta) = a\eta + b$, linearity leads to:

$$\int d\eta f(\eta + c) = \int d\eta(a\eta + b) + ac\int d\eta = \int d\eta f(\eta) + ac\int d\eta \tag{A.57}$$

which, given translational invariance, implies

$$\int d\eta = 0 \tag{A.58}$$

We also define the normalization

$$\int d\eta\eta = 1 \tag{A.59}$$

Now, introduce annihilation $\hat{a}$ and creation operators $\hat{a}^\dagger$ obeying the anticommutation relation:

$$\{\hat{a}, \hat{a}^\dagger\} = 1 \ \ , \ \ \hat{a}^2 = \left(\hat{a}^\dagger\right)^2 = 0 \tag{A.60}$$

These operators act on a two dimensional Hilbert space. A basis in this space is given by states $|0\rangle$ and $|1\rangle$, defined by $|1\rangle = a^\dagger|0\rangle$ and $a|0\rangle = 0$. They are supposed normalized: $\langle 0|0\rangle = 1$ and $\langle 1|1\rangle = 1$. From their definition and the anticommutation relations, they are also orthonormal, $\langle 0|1\rangle = 0$.

Next, we consider the Grassmann algebra generated by two variables η and η^*.

With these, we construct fermionic coherent states in analogy with bosonic coherent states, namely:

$$|\eta\rangle \equiv e^{-\eta\hat{a}^\dagger}|0\rangle = (1-\eta\hat{a}^\dagger)|0\rangle = |0\rangle - \eta|1\rangle \tag{A.61}$$

$$\langle\eta| \equiv \langle 0|e^{-\hat{a}\eta^*} = \langle 0|(1-\hat{a}\eta^*) = \langle 0| - \langle 1|\eta^* \tag{A.62}$$

From the normalization of the states $|0\rangle$ and $|1\rangle$ and the Grassmann number nature of η and η^*, we have that the coherent states satisfy the following properties:

$$\langle\eta|0\rangle = \langle 0|\eta\rangle = 1 \;\;,\;\; \langle 1|\eta\rangle = \langle\eta|1\rangle^* = -\eta \tag{A.63}$$

From these, we can derive the normalization of the coherent state $|\eta\rangle$:

$$\begin{aligned}\langle\eta|\eta\rangle &= \langle 0|0\rangle - \eta\langle 0|1\rangle - \langle 1|0\rangle\eta^* + \eta^*\eta\langle 1|1\rangle \\ &= 1 + \eta^*\eta = e^{\eta^*\eta}\end{aligned} \tag{A.64}$$

We can also derive a completeness relation that the coherent state $|\eta\rangle$ satisfies:

$$\begin{aligned}\int d\eta^* d\eta\, e^{-\eta^*\eta}\,|\eta\rangle\langle\eta| &= \int d\eta^* d\eta\, e^{-\eta^*\eta}\, e^{-\eta\hat{a}^\dagger}|0\rangle\langle 0|e^{-\hat{a}\eta^*} \\ &= \int d\eta^* d\eta\,(1-\eta^*\eta)\,(1-\eta\hat{a}^\dagger)|0\rangle\langle 0|(1-\hat{a}\eta^*) \\ &= \int d\eta^* d\eta\;(1-\eta^*\eta) \\ &\times\left(|0\rangle\langle 0| - |0\rangle\langle 1|\eta^* - \eta|1\rangle\langle 0| + |1\rangle\langle 1|\eta\eta^*\right) \\ &= |0\rangle\langle 0|\left(-\int d\eta^* d\eta\,\eta^*\eta\right) + |1\rangle\langle 1|\left(\int d\eta^* d\eta\,\eta\eta^*\right) \\ &= |0\rangle\langle 0| + |1\rangle\langle 1| = \mathbb{I}\end{aligned} \tag{A.65}$$

where we used the results (A.58) and (A.59). In addition, one can use the coherent state to compute the trace of an operator $\hat{A}$ defined in this two-dimensional Hilbert space and written in terms of the creation and annihilation operators, namely:

$$\begin{aligned}\int d\eta^* d\eta\, e^{-\eta^*\eta}\,\langle -\eta|A|\eta\rangle &= \int d\eta^* d\eta\;(1-\eta^*\eta) \\ &\times\left(\langle 0|\hat{A}|0\rangle + \eta^*\langle 1|\hat{A}|0\rangle - \eta\langle 0|\hat{A}|1\rangle - \eta^*\eta\langle 1|\hat{A}|1\rangle\right) \\ &= \langle 0|A|0\rangle\left(-\int d\eta^* d\eta\;\eta^*\eta\right) + \langle 1|A|1\rangle\left(-\int d\eta^* d\eta\,\eta^*\eta\right) \\ &= \langle 0|\hat{A}|0\rangle + \langle 1|\hat{A}|1\rangle = \mathrm{Tr}\hat{A}\end{aligned} \tag{A.66}$$

In view of the possibility of using the coherent state to compute the the trace of an operator and the completeness relation of the coherent state, one can obtain a functional integral representation for the partition function for an Hamiltonian written in terms of the creation and annihilation operators. For example, for an Hamiltonian of the form

$$\hat{H} = \omega\, \hat{a}^\dagger \hat{a} \tag{A.67}$$

we have

$$\mathcal{Z} = \mathrm{Tr}\, e^{-\beta \hat{H}} = \int d\eta^* d\eta\; e^{-\eta^*\eta}\; \langle -\eta | e^{-\beta\hat{H}} | \eta \rangle \tag{A.68}$$

Now, one can proceed as in the case of boson fields, discretize β and insert the identity from Eq. (A.65) into Eq. (A.68) at the appropriate places.

This will lead us to terms of the form:

$$\begin{aligned} e^{-\eta^*_{i+1}\eta_{i+1}} \langle \eta_{i+1} | e^{-\epsilon \hat{H}(\hat{a}^\dagger, \hat{a})} | \eta_i \rangle &= e^{\eta^*_{i+1}\eta_{i+1}}\; \langle \eta^*_{i+1} | \eta_i \rangle\; e^{-\epsilon H(\eta^*_{i+1}, \eta_i)} \\ &= e^{-\eta^*_{i+1}\eta_{i+1} + \eta^*_{i+1}\eta_i - \epsilon H(\eta^*_{i+1}, \eta_i)} \\ &= e^{-\epsilon\left[\eta^*_{i+1}(\eta_{i+1}-\eta_i)/\epsilon + H(\eta^*_{i+1}, \eta_i)\right]} \end{aligned} \tag{A.69}$$

Next, consider a typical term that appears in Eq.(A.68). Taking $\eta \equiv \eta_1$, one obtains:

$$\begin{aligned} &\int d\eta_1^* d\eta_1 e^{-\eta_1^*\eta_1} \langle -\eta_1 | e^{-\epsilon \hat{H}(\hat{a}^\dagger, \hat{a})} | \int d\eta_N^* d\eta_N | \eta_N \rangle \\ &= \int d\eta_1^* d\eta_1 \int d\eta_N^* d\eta_N \exp\left[-\eta_1^*\eta_1 - \eta_1^*\eta_N - \epsilon H(-\eta_1^*, \eta_N)\right] \\ &= \int d\eta_1^* d\eta_1 \int d\eta_N^* d\eta_N \exp\left\{-\epsilon\left[\eta_1^* \frac{\eta_1 + \eta_N}{\epsilon} + H(-\eta_1^*, \eta_1)\right]\right\} \\ &= \int d\eta_1^* d\eta_1 \int d\eta_N^* d\eta_N \exp\left\{-\epsilon\left[-\eta_1^* \frac{-\eta_1 - \eta_N}{\epsilon} + H(-\eta_1^*, \eta_1)\right]\right\} \end{aligned} \tag{A.70}$$

and thus

$$\int d\eta_N^* d\eta_N \cdots \int d\eta_1^* d\eta_1 \exp\left\{-\epsilon \sum \left[\eta^*_{i+1} \frac{\eta_{i+1} - \eta_1}{\epsilon} + H(\eta^*_{i+1}, \eta_i)\right]_{\eta_{N+1} \equiv -\eta_1}\right\} \tag{A.71}$$

At last, taking the limit $N \to \infty$, $\epsilon \to 0$, with $\beta = \epsilon N$ kept constant, we arrive at,

$$\mathcal{Z} = \int_{\eta^*(\beta) = -\eta^*(0)} \mathcal{D}\eta^* \int_{\eta(\beta) = -\eta(0)} \mathcal{D}\eta \exp\left(-\int_0^\beta d\tau [\eta^* \partial_\tau \eta + H(\eta^*, \eta)]\right) \tag{A.72}$$

We also need a Gaussian functional integral with Grassmann variabled. For a single Grassmann variable, we have:

$$\int d\eta^* d\eta e^{-\eta^* b \eta} = \int d\eta^* d\eta (1 - \eta^* b \eta) = \int d\eta^* d\eta (1 + \eta \eta^* b) = b \qquad \text{(A.73)}$$

A multidimensional integral is of the form

$$I = \left(\prod_i \int d\eta_i^* d\eta_i \right) e^{-\eta_i^* B_{ij} \eta_j} \qquad \text{(A.74)}$$

where B is a hermitian matrix with eigenvalues b_i. We can rotate the η_i's and the η_i^*'s by a unitary transformation that diagonalizes B, defined by

$$\begin{aligned} \eta_i^* &\rightarrow U_{ki}^* \eta_k^{*'} \\ \eta_i &\rightarrow U_{jl} \eta_l' \end{aligned} \qquad \text{(A.75)}$$

Then, we can then write

$$\begin{aligned} I &= \left(\prod_i \int d\eta_i^* d\eta_i \right) e^{-\sum_i \eta_i^* b_i \eta_j} = \left(\prod_i \int d\eta_i^* d\eta_i e^{-\eta_i^* b_i \eta_j} \right) \\ &= \prod_i b_i = \det B \end{aligned} \qquad \text{(A.76)}$$

A.3 Partition function for fermionic fields

Now, let us move on to discussing the fermionic fields. To begin characterizing a system containing non-interacting fermions of mass m, we commence with the lagrangian,

$$\mathcal{L}_0 = \overline{\psi}(i\gamma^\mu \partial_\mu - m)\psi \qquad \text{(A.77)}$$

where $\overline{\psi} = \psi^\dagger \gamma^0$. We aim to introduce a chemical potencial into this Lagrangian. To achieve this, we ascertain the conserved current: initially identifying the global symmetry of the lagrangian by the transformations $\psi \rightarrow e^{-i\alpha}$. This yields the conserved current:

$$j^\mu = \frac{\partial \mathcal{L}_0}{\partial(\partial_\mu \psi)} \frac{\delta \psi}{\delta \alpha} = \overline{\psi} \gamma^\mu \psi \qquad \text{(A.78)}$$

so, the conserved charge is,

$$j^0 = \psi^\dagger \underbrace{\gamma^0\gamma^0}_{\mathbb{I}} \psi = \psi^\dagger\psi \tag{A.79}$$

The conjugate momentum is

$$\Pi = \frac{\partial \mathcal{L}_0}{\partial(\partial_0\psi)} = i\psi^\dagger \tag{A.80}$$

In this case, we must therefore treat the fermionic fields as independent variables. The partition function for the fermions is:

$$\begin{aligned} \mathcal{Z} &= \mathrm{Tr} e^{-\beta(\hat{H}-\mu\hat{N})} \\ &= \int_{\text{antiperiodic}} \mathcal{D}\psi^\dagger \mathcal{D}\psi \exp\left[-\int_{\mathbf{x}} (\mathcal{H} - \mu\mathcal{N} - i\Pi\partial_\tau\psi)\right] \end{aligned} \tag{A.81}$$

It is important to recall that the periodicity observed in bosonic fields stems from the trace taken within the operator formalism. Simply put, the partition function in the path integral formalism can be deduced from a transition amplitude featuring identical initial and final states. However, for fermions, the fields in the path integral are Grassmann variables due to the anticommutation relations of creation and annihilation operators. Consequently, the trace involves a transition amplitude where the initial and final states differ by a sign. As a result, the fermionic partition function involves integration over antiperiodic fields $\psi(0,\mathbf{x}) = -\psi(\beta,\mathbf{x})$ and $\psi^\dagger(0,\mathbf{x}) = -\psi^\dagger(\beta,\mathbf{x})$.

With the Hamiltonian:

$$\begin{aligned} \mathcal{H} &= \Pi\partial_0\psi - \mathcal{L}_0 = \Pi\partial_0\psi - \overline{\psi}(i\gamma^\mu\partial_\mu - m)\psi \\ &= i\psi^\dagger\partial_0\psi - i\psi^\dagger\partial_0\psi + i\overline{\psi}\gamma\cdot\nabla\psi + \overline{\psi}m\psi \\ &= \overline{\psi}(i\gamma\cdot\nabla + m)\psi \end{aligned} \tag{A.82}$$

and taking the exponential term of the partition function Eq.(A.81), we have

$$\mathcal{L}_{0E} = \overline{\psi}(i\gamma^\mu\partial_\mu + \gamma^0\mu - m)\psi \tag{A.83}$$

where $\mathcal{L}_{0E}$ is the Lagrangian density in Euclidean space, for which $i\gamma^\mu\partial_\mu = -\gamma^0\partial_\tau - i\gamma\cdot\nabla$. Observe that, once more, the chemical potential enters like the temporal component of a gauge field, establishing coupling with the fermions.

Now, similar to the scenario with bosons, we introduce the Fourier - transformed fields

$$\psi(X) = \frac{1}{\sqrt{V}} \sum_K e^{-iK\cdot X} \psi(K) \quad , \quad \overline{\psi}(X) = \frac{1}{\sqrt{V}} \sum_K e^{iK\cdot X} \overline{\psi}(K) \tag{A.84}$$

Once more, using $k_0 = -i\omega_n$ to express $K\cdot X$ as $-(\omega_n \tau + \mathbf{k}\cdot\mathbf{x})$. Now, the antiperiodicity condition, $\psi(0,\mathbf{x}) = -\psi(\beta,\mathbf{x})$, implies $e^{i\omega_n\beta} = -1$, leading to the fermionic Matsubara frequencies as follows:

$$\omega_n = (2n+1)\pi T \quad , \quad n \in \mathbb{Z} \tag{A.85}$$

Hence, it follows that:

$$\begin{aligned} I &= \int_{\mathbf{x}} \overline{\psi}(-\gamma^0 \partial_\tau - i\boldsymbol{\gamma}\cdot\boldsymbol{\nabla} + \gamma^0\mu - m)\psi \\ &= \int_{\mathbf{x}} \frac{1}{V} \sum_K e^{iK\cdot X} \overline{\psi}(K) \left[-\gamma^0\partial_\tau - i\boldsymbol{\gamma}\cdot\boldsymbol{\nabla} + \gamma^0\mu - m \right] \sum_{K'} e^{-iK'\cdot X} \psi(K) \end{aligned} \tag{A.86}$$

and similarly to what was done for bosonic fields, we will have the following result:

$$\begin{aligned} I &= \sum_K \left[\overline{\psi}(K)\gamma^\mu K_\mu \psi(K) + \overline{\psi}(K)\gamma^0\mu\psi(K) - \overline{\psi}(K) m \psi(K) \right] \\ &= -\sum_K \overline{\psi}(K) \frac{G_0^{-1}}{T} \psi(K) \end{aligned} \tag{A.87}$$

where

$$G_0^{-1}(K) = -\gamma^\mu K_\mu - \gamma^0\mu + m \tag{A.88}$$

is the free inverse fermion propagator in momentum space.

Given the Dirac matrices :

$$\gamma^0 = \begin{pmatrix} \mathbb{I}_2 & 0 \\ 0 & -\mathbb{I}_2 \end{pmatrix} \text{ and } \boldsymbol{\gamma} = \begin{pmatrix} 0 & \boldsymbol{\sigma} \\ -\boldsymbol{\sigma} & 0 \end{pmatrix} \tag{A.89}$$

where $\mathbb{I}_2$ represents 2×2 identity matrices and $\boldsymbol{\sigma} = \sigma^i = (\sigma^x, \sigma^y, \sigma^z)$ represents the Pauli matrices, we can express $G_0^{-1}(K)$ in a 4×4 matrix form:

$$G_0^{-1} = \begin{pmatrix} -(k_0+\mu)+m & -\boldsymbol{\sigma}\cdot\mathbf{k} \\ \boldsymbol{\sigma}\cdot\mathbf{k} & (k_0+\mu)+m \end{pmatrix} \tag{A.90}$$

and given that these fields are Grassmann variables, from Eq.(A.76):

$$\int \prod_k^N d\eta_k^\dagger d\eta_k \exp\left(-\sum_{i,j}^N \eta_i^\dagger D_{ij}\eta_j\right) = \det D \tag{A.91}$$

we arrive at the following partition function

$$\mathcal{Z} = \det \frac{G_0^{-1}(K)}{T} = \det \frac{1}{T}\begin{pmatrix} -(k_0+\mu)+m & -\boldsymbol{\sigma}\cdot\mathbf{k} \\ \boldsymbol{\sigma}\cdot\mathbf{k} & (k_0+\mu)+m \end{pmatrix} \tag{A.92}$$

In order to solve this determinant, we can use the general formula

$$\det\begin{pmatrix} A & B \\ C & D\end{pmatrix} = \det(AD - B^{-1}CD) \tag{A.93}$$

to obtain

$$\det \frac{G_0^{-1}(K)}{T} = \prod_k \left(\frac{k^2+m^2-(k_0+\mu)^2}{T^2}\right)^2 \tag{A.94}$$

with $(\boldsymbol{\sigma}\cdot\mathbf{k})^2 = k^2$. And then, knowing that $k_0 = -i\omega_n$, we have

$$\ln\mathcal{Z} = \sum_k \ln\left(\frac{E_k^2+(\omega_n+i\mu)^2}{T^2}\right)^2 \quad , \quad E_k \equiv \sqrt{k^2+m^2} \tag{A.95}$$

and so

$$\begin{aligned}\ln\mathcal{Z} &= \sum_k\left(\ln\frac{E_k^2+(\omega_n+i\mu)^2}{T^2} + \ln\frac{E_k^2+(-\omega_n+i\mu)^2}{T^2}\right) \\ &= \sum_k\left(\ln\frac{\omega_n^2+(E_k-\mu)^2}{T^2} + \ln\frac{\omega_n^2+(E_k+\mu)^2}{T^2}\right)\end{aligned} \tag{A.96}$$

In the first step, we replaced ω_n by $-\omega_n$, as the result of the sum remains the same since the sum is taken over the entire $n \in \mathbb{Z}$. And in the second step, we can verify that:

$$[E_k^2+(\omega_n+i\mu)^2][E_k^2+(-\omega_n+i\mu)^2] = [\omega_n^2+(E_k-\mu)^2][\omega_n^2+(E_k+\mu)^2]$$

The next step now is to perform the sum over the fermionic Matsubara frequencies. So, similar to what has already been done for the bosonic case, we have

$$\sum_n \ln\frac{\omega_n^2+E_k^2}{T^2} = \frac{E_k}{T} + 2\ln\left(1+e^{-E_k/T}\right) + C \tag{A.97}$$

A.3.1 Summation Over Fermionic Matsubara Frequencies

Consider the following equality

$$\begin{aligned} I &= \sum_n \ln \frac{\omega_n^2 + \epsilon_k^2}{T^2} \\ &= \int_1^{(\epsilon_k/T)^2} dx^2 \sum_n \frac{1}{(2n+1)^2\pi^2 + x^2} + \sum_n \ln\left[1 + (2n+1)^2\pi^2\right] \end{aligned} \tag{A.98}$$

For bosonic fields, we used the coth to express the sum in terms of a contour integral but now use we use the tanh,

$$T \sum \frac{1}{\omega_n^2 + \epsilon_k^2} = -\frac{1}{2\pi i} \oint_c d\omega \frac{1}{\omega^2 - \epsilon_k^2} \frac{1}{2} \tanh \frac{\omega}{2T} \tag{A.99}$$

which can also be easily shown using the residue theorem: The poles of tanh are such that its denominator, $e^{\omega/2T} + e^{-\omega/2T}$, equals zero

$$e^{\omega/2T} + e^{-\omega/2T} = 0 \tag{A.100}$$

hence, $\omega/2T$ must be an odd integer multiple of $i\pi/2$, i.e.

$$\frac{\omega}{2T} = (2n+1)\frac{i\pi}{2} \quad \Rightarrow \quad \omega = i\omega_n \tag{A.101}$$

then

$$\begin{aligned} \phi(i\omega_n) &= \frac{1}{2} \frac{e^{i\omega_n/2T} - e^{-i\omega_n/2T}}{-\omega_n^2 - \epsilon_k^2} = -i\frac{\sin(\omega_n/2T)}{\omega_n^2 + \epsilon_k^2} \\ &= -i\frac{(-1)^n}{\omega_n^2 + \epsilon_k^2} \end{aligned} \tag{A.102}$$

and

$$\begin{aligned} \psi'(i\omega_n) &= \frac{d}{d\omega}(e^{\omega/2T} + e^{-\omega/2T})\big|_{\omega = i\omega_n} = \frac{1}{2T}\left(e^{i\omega_n/2T} - e^{-i\omega_n/2T}\right) \\ &= i\frac{(-1)^n}{T} \end{aligned} \tag{A.103}$$

Finally, it is evident that all of this confirms Eq.(A.99). Now, similarly to what was done for bosons, we have

$$T\sum_n \frac{1}{\omega_n^2+\epsilon_k^2} = -\frac{1}{2\pi i}\int_{-i\infty+\eta}^{i\infty+\eta} d\omega \frac{1}{\omega^2-\epsilon_k^2}\tanh\frac{\omega}{2T} \tag{A.104}$$

Reapplying the residue theorem by closing the contour in the positive half-plane, we obtain

$$\phi(\omega) = \tanh\frac{\omega}{2T} \quad , \quad \psi(\omega) = \omega^2-\epsilon_k^2 \quad , \quad \psi'(\omega) = 2\omega \tag{A.105}$$

with the pole $\omega = +\epsilon$. Threrefore, we have that

$$\begin{aligned} T\sum_n \frac{1}{\omega_n^2+\epsilon_k^2} &= \frac{1}{2\epsilon_k}\tanh\frac{\epsilon_k}{2T} = \frac{1}{2\epsilon_k}\left(\frac{e^{\epsilon_k/2T}-e^{-\epsilon_k/2T}}{e^{\epsilon_k/T}+e^{-\epsilon_k/T}}\right) \\ &= \frac{1}{2\epsilon_k}\left[\frac{e^{-\epsilon_k/2T}}{e^{-\epsilon_k/2T}}\left(\frac{e^{\epsilon_k/T}-1}{e^{\epsilon_k/T}+1}\right)\right] = \frac{1}{2\epsilon_k}[1-2f_F(\epsilon_k)] \end{aligned} \tag{A.106}$$

where

$$f_F(\epsilon) = \frac{1}{e^{\epsilon/T}+1} \tag{A.107}$$

is the Fermi distribution.

Substituting this result into Eq.(A.98):

$$\sum_n \ln\left[\frac{\omega_n^2+\epsilon_k^2}{T^2}\right] = \int_1^{(\epsilon/T)^2} dx^2\,\frac{1}{x}\left(\frac{1}{2}-\frac{1}{e^x+1}\right)+C \tag{A.108}$$

Let us work on the integral:

$$\begin{aligned} 2\int du\left(\frac{1}{2}-\frac{1}{e^u+1}\right) &= 2\int du\left(\frac{1}{2}+\frac{e^u}{e^u+1}-1\right) \\ &= \int du\left(\frac{2e^u}{e^u+1}-1\right) = 2\int dw\,\frac{1}{w}-\int du \\ &= 2\ln\left(e^u+1\right)-u = 2\ln\left(\frac{1+e^{-u}}{e^{-u}}\right)-u \\ &= -2\ln\left(e^{-u}\right)+2\ln\left(1+e^{-u}\right)-u \\ &= u+2\ln\left(1+e^{-u}\right) \end{aligned} \tag{A.109}$$

Evaluating the integral in the appropriate limits, we obtain

$$\sum_n \ln\frac{\omega_n^2+\epsilon_k^2}{T^2} = \frac{\epsilon_k}{T}+2\ln\left(1+e^{-\epsilon_k/T}\right)+C \tag{A.110}$$

Bibliography

[1] C. E. Rhoades Jr and R. Ruffini, “Maximum mass of a neutron star,” *Physical Review Letters*, vol. 32, no. 6, p. 324, 1974.

[2] S. Bahcall, B. W. Lynn, and S. B. Selipsky, “Are neutron stars q-stars?,” *Nuclear Physics B*, vol. 331, no. 1, pp. 67–79, 1990.

[3] P. Negi and M. Durgapal, “Stable ultracompact objects and an upper bound on neutron star masses,” *Astronomy and Astrophysics, v. 353, p. 641-645 (2000)*, vol. 353, pp. 641–645, 2000.

[4] J. R. Oppenheimer and G. M. Volkoff, “On massive neutron cores,” *Physical Review*, vol. 55, no. 4, p. 374, 1939.

[5] S. Chandrasekhar and V. Ferrari, “On the non-radial oscillations of a star. iii. a reconsideration of the axial modes,” *Proceedings of the Royal Society of London. Series A: Mathematical and Physical Sciences*, vol. 434, no. 1891, pp. 449–457, 1991.

[6] A. Hewish, S. J. Bell, J. D. Pilkington, P. Frederick Scott, and R. A. Collins, “Observation of a rapidly pulsating radio source,” in *A Source Book in Astronomy and Astrophysics, 1900–1975*, pp. 498–504, Harvard University Press, 1979.

[7] J. Comella, H. Craft, R. Lovelace, J. Sutton, and G. L. Tyler, “Crab nebula pulsar np 0532,” *Nature*, vol. 221, no. 5179, pp. 453–454, 1969.

[8] B. P. Abbott, R. Abbott, T. Abbott, F. Acernese, K. Ackley, C. Adams, T. Adams, P. Addesso, R. Adhikari, V. B. Adya, *et al.*, “Gw170817: observation of gravitational waves from a binary neutron star inspiral,” *Physical review letters*, vol. 119, no. 16, p. 161101, 2017.

[9] V. Cardoso and P. Pani, “Testing the nature of dark compact objects: a status report,” *Living Reviews in Relativity*, vol. 22, pp. 1–104, 2019.

[10] A. Urbano and H. Veermäe, “On gravitational echoes from ultracompact exotic stars,” *Journal of Cosmology and Astroparticle Physics*, vol. 2019, no. 04, p. 011, 2019.

[11] M. Mannarelli and F. Tonelli, "Gravitational wave echoes from strange stars," *Physical Review D*, vol. 97, no. 12, p. 123010, 2018.

[12] C. Zhang, "Gravitational wave echoes from interacting quark stars," *Physical Review D*, vol. 104, no. 8, p. 083032, 2021.

[13] J. Piekarewicz, "Relativistic density functional theory for finite nuclei and neutron stars," in *Relativistic Density Functional for Nuclear Structure*, pp. 625–658, World Scientific, 2016.

[14] M. Kortelainen, T. Lesinski, J. Moré, W. Nazarewicz, J. Sarich, N. Schunck, M. Stoitsov, and S. Wild, "Nuclear energy density optimization," *Physical Review C*, vol. 82, no. 2, p. 024313, 2010.

[15] T. Editors, "Editorial: Uncertainty estimates," *Phys. Rev. A*, vol. 83, p. 040001, Apr 2011.

[16] J. D. Walecka, "A theory of highly condensed matter," *Annals of Physics*, vol. 83, no. 2, pp. 491–529, 1974.

[17] B. D. Serot, "A relativistic nuclear field theory with π and ρ mesons," *Physics Letters B*, vol. 86, no. 2, pp. 146–150, 1979.

[18] P. Hohenberg and W. Kohn, "Inhomogeneous electron gas," *Phys. Rev.*, vol. 136, pp. B864–B871, Nov 1964.

[19] W. Kohn and L. J. Sham, "Self-consistent equations including exchange and correlation effects," *Phys. Rev.*, vol. 140, pp. A1133–A1138, Nov 1965.

[20] W. Kohn, "Nobel lecture: Electronic structure of matter—wave functions and density functionals," *Rev. Mod. Phys.*, vol. 71, pp. 1253–1266, Oct 1999.

[21] G. a. Krein, "Review of hadrons in medium," *AIP Conf. Proc.*, vol. 1701, no. 1, p. 020012, 2016.

[22] G. Krein and T. A. J. Maris, "Compatibility of the nuclear shell and nucleon bag models," *Phys. Rev. C*, vol. 36, pp. 365–371, 1987.

[23] G. Röpke, D. Blaschke, and H. Schulz, "Pauli quenching effects in a simple string model of quark/nuclear matter," *Physical Review D*, vol. 34, no. 11, p. 3499, 1986.

[24] D. Blaschke and G. Röpke, "Pauli-quenching for hadrons in nuclear matter-a quark substructure effect," tech. rep., Joint Inst. for Nuclear Research, 1988.

[25] M. E. Bracco, G. Krein, and M. Nielsen, "Quark meson coupling model with constituent quarks: Exchange and pionic effects," *Phys. Lett. B*, vol. 432, pp. 258–265, 1998.

[26] D. Hadjimichef, G. Krein, S. Szpigel, and J. S. da Veiga, "Mapping of composite hadrons into elementary hadrons and effective hadronic Hamiltonians," *Annals Phys.*, vol. 268, pp. 105–148, 1998.

[27] G. Krein and V. E. Vizcarra, "Equation of state of quark nuclear matter," in *Joint CSSM / JHF / NITP Workshop on Physics at the Japan Hadron Facility*, 6 2002.

[28] D. Blaschke, H. Grigorian, and G. Röpke, "Chirally improved quark pauli blocking in nuclear matter and applications to quark deconfinement in neutron stars," *Particles*, vol. 3, no. 2, p. 33, 2020.

[29] T. Kojo, G. Baym, and T. Hatsuda, "Implications of NICER for Neutron Star Matter: The QHC21 Equation of State," *Astrophys. J.*, vol. 934, no. 1, p. 46, 2022.

[30] E. Fonseca, H. T. Cromartie, T. T. Pennucci, P. S. Ray, A. Y. Kirichenko, S. M. Ransom, P. B. Demorest, I. H. Stairs, Z. Arzoumanian, L. Guillemot, *et al.*, "Refined mass and geometric measurements of the high-mass psr j0740+ 6620," *The Astrophysical Journal Letters*, vol. 915, no. 1, p. L12, 2021.

[31] F. Özel and P. Freire, "Masses, radii, and the equation of state of neutron stars," *Annual Review of Astronomy and Astrophysics*, vol. 54, pp. 401–440, 2016.

[32] R. C. Tolman, "Static solutions of einstein's field equations for spheres of fluid," *Physical Review*, vol. 55, no. 4, p. 364, 1939.

[33] L. Woltjer, "X-rays and type i supernova remnants.," *The Astrophysical Journal*, vol. 140, pp. 1309–1313, 1964.

[34] R. A. Hulse and J. H. Taylor, "Discovery of a pulsar in a binary system," *The Astrophysical Journal*, vol. 195, pp. L51–L53, 1975.

[35] F. Pacini, "Energy emission from a neutron star," *Nature*, vol. 216, no. 5115, pp. 567–568, 1967.

[36] T. Gold, "Rotating neutron stars as the origin of the pulsating radio sources," *Nature*, vol. 218, no. 5143, pp. 731–732, 1968.

[37] A. Cameron, "Neutron star models.," *Astrophysical Journal, vol. 130, p. 884*, vol. 130, p. 884, 1959.

[38] V. Pandharipande, "Hyperonic matter," *Nuclear Physics A*, vol. 178, no. 1, pp. 123–144, 1971.

[39] H. Bethe and M. Johnson, "Dense baryon matter calculations with realistic potentials," *Nuclear Physics A*, vol. 230, no. 1, pp. 1–58, 1974.

[40] S. A. Moszkowski, "Energy of neutron-star matter," *Physical Review D*, vol. 9, no. 6, p. 1613, 1974.

[41] N. K. Glendenning, "Neutron stars are giant hypernuclei?," *Astrophysical Journal, Part 1 (ISSN 0004-637X), vol. 293, June 15, 1985, p. 470-493.*, vol. 293, pp. 470–493, 1985.

[42] N. K. Glendenning, "Nuclear and particle astrophysics," *Proc. Int. Summer School on the Structure of Hadrons and Hadronic Matter, Dronten, Netherlands*, p. 275, 1990.

[43] N. K. Glendenning, "THE HYPERON COMPOSITION OF NEUTRON STARS," *Phys. Lett. B*, vol. 114, pp. 392–396, 1982.

[44] N. Glendenning and S. Moszkowski, "Reconciliation of neutron-star masses and binding of the λ in hypernuclei," *Physical review letters*, vol. 67, no. 18, p. 2414, 1991.

[45] N. Glendenning, "Neutron-star masses as a constraint on the nuclear compression modulus," *Physical Review Letters*, vol. 57, no. 9, p. 1120, 1986.

[46] N. K. Glendenning, "Equation of state from nuclear and astrophysical evidence," *Physical Review C*, vol. 37, no. 6, p. 2733, 1988.

[47] N. Glendenning, "Fast pulsars, variational bounds, other facets of compact stars," *Nuclear Physics B-Proceedings Supplements*, vol. 24, no. 2, pp. 110–118, 1991.

[48] N. K. Glendenning, "First-order phase transitions with more than one conserved charge: Consequences for neutron stars," *Physical Review D*, vol. 46, no. 4, p. 1274, 1992.

[49] N. K. Glendenning, *Compact stars: Nuclear physics, particle physics and general relativity*. Springer Science & Business Media, 2012.

[50] R. Nandi and D. Bandyopadhyay, "Magnetised neutron star crusts and torsional shear modes of magnetars," in *Journal of Physics: Conference Series*, vol. 420, p. 012144, IOP Publishing, 2013.

[51] L. Rezzolla, P. Pizzochero, D. I. Jones, N. Rea, I. Vidaña, *et al.*, *The physics and astrophysics of neutron stars*, vol. 457. Springer, 2018.

[52] H. T. Cromartie, E. Fonseca, S. M. Ransom, P. B. Demorest, Z. Arzoumanian, H. Blumer, P. R. Brook, M. E. DeCesar, T. Dolch, J. A. Ellis, *et al.*, "Relativistic shapiro delay measurements of an extremely massive millisecond pulsar," *Nature Astronomy*, vol. 4, no. 1, pp. 72–76, 2020.

[53] J. H. Taylor and J. M. Weisberg, "A new test of general relativity-gravitational radiation and the binary pulsar psr 1913+ 16," *Astrophysical Journal, Part 1, vol. 253, Feb. 15, 1982, p. 908-920. NSF-supported research.*, vol. 253, pp. 908–920, 1982.

[54] A. Schmitt, *Dense matter in compact stars: A pedagogical introduction*. Springer, 2010.

[55] M. Le Bellac, *Thermal field theory*. Cambridge university press, 2000.

[56] R. W. Romani, D. Kandel, A. V. Filippenko, T. G. Brink, and W. Zheng, "Psr j0952- 0607: the fastest and heaviest known galactic neutron star," *The Astrophysical Journal Letters*, vol. 934, no. 2, p. L17, 2022.

[57] R. L. Workman *et al.*, "Review of Particle Physics," *Progress of Theoretical and Experimental Physics*, vol. 2022, p. 083C01, 08 2022.

[58] F. Myhrer and J. Wroldsen, "The Nucleon-nucleon Force and the Quark Degrees of Freedom," *Rev. Mod. Phys.*, vol. 60, p. 629, 1988.

[59] A. Fetter and J. Walecka, *Quantum Theory of Many-particle Systems*. Dover Books on Physics, Dover Publications, 2003.

[60] P. A. M. Guichon, "A Possible Quark Mechanism for the Saturation of Nuclear Matter," *Phys. Lett. B*, vol. 200, pp. 235–240, 1988.

[61] K. Saito, K. Tsushima, and A. W. Thomas, "Nucleon and hadron structure changes in the nuclear medium and impact on observables," *Prog. Part. Nucl. Phys.*, vol. 58, pp. 1–167, 2007.

[62] J. I. Kapusta and C. Gale, *Finite-temperature field theory: Principles and applications*. Cambridge Monographs on Mathematical Physics, Cambridge University Press, 2011.

[63] A. Schmitt, "Thermal field theory, ws08/09," *Lecture at Vienna University of Technology*, 2009.